



Contents lists available at ScienceDirect

Chemical Engineering Journal

journal homepage: [www.elsevier.com/locate/cej](http://www.elsevier.com/locate/cej)

## Synergistic effect of TiO<sub>2</sub> photocatalytic advanced oxidation processes in the treatment of refinery effluents

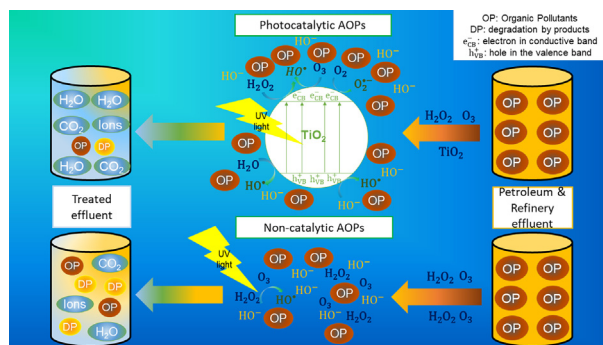
André Fernandes<sup>a</sup>, Patrycja Makos<sup>a</sup>, Zhaohui Wang<sup>b,c</sup>, Grzegorz Boczkaj<sup>a,\*</sup>

<sup>a</sup> Gdansk University of Technology, Faculty of Chemistry, Department of Process Engineering and Chemical Technology, 80 – 233 Gdansk, G. Narutowicza St. 11/12, Poland

<sup>b</sup> Shanghai Key Lab for Urban Ecological Processes and Eco-Restoration, School of Ecological and Environmental Sciences, East China Normal University, Shanghai 200241, China

<sup>c</sup> Institute of Eco-Chongming (IEC), Shanghai 200062, China

### GRAPHICAL ABSTRACT



### ARTICLE INFO

#### Keywords:

Hydroxyl radicals  
Wastewater treatment  
Photocatalysis  
AOP  
TiO<sub>2</sub>  
Ozone

### ABSTRACT

Different types of photolytic and photocatalytic advanced oxidation processes (AOPs) were used for treatment of refinery effluents from bitumen production. The treatment efficiency was evaluated by analyzing chemical oxygen demand (COD), biological oxygen demand (BOD<sub>5</sub>), volatile organic compounds (VOCs) and sulfide ions concentration. The studies revealed a synergistic effect of application of external oxidants (O<sub>3</sub>, H<sub>2</sub>O<sub>2</sub>, O<sub>3</sub>/H<sub>2</sub>O<sub>2</sub>) with TiO<sub>2</sub> and UV applied for improved COD and BOD<sub>5</sub> reduction as well as the degradation of the VOCs present in the effluents. Among studied processes a photocatalytic process combined with peroxone (TiO<sub>2</sub>/UV/O<sub>3</sub>/H<sub>2</sub>O<sub>2</sub>) was the optimal and the most economical technology. It allows to reduce 38 and 32% of COD and BOD<sub>5</sub> respectively and degrade 84% of total VOCs in 280 min of treatment. At this conditions the reduced COD exceeds over 30% a theoretical value based on the dose of oxidants, which proves the importance of photocatalysis in the developed technology. The sulfide ions were completely depleted in all experiments in the first 30 min of treatment. The addition of TiO<sub>2</sub> in the AOPs technology revealed a decrease in the process cost using less amount

**Abbreviations:** AOPs, Advanced Oxidation Processes; CD, conductive band; DLLME, dispersive liquid-liquid microextraction; e<sup>-</sup>, electron; GC-MS/FPD, NPD, gas chromatography-mass spectrometry/flame photometric detector/nitrogen phosphorus detector; HO<sup>•</sup>, hydroxyl radicals; h<sub>VB</sub><sup>+</sup>, holes in the VB; O<sub>3</sub>/H<sub>2</sub>O<sub>2</sub>, peroxone; O-VOCs, oxygen volatile organic compounds; PZC, point of zero charge; rpm, rotations per minute; RSD, relative standard deviation; TiO<sub>2</sub>, titanium dioxide; TiO<sub>2</sub>/UV, photocatalytic TiO<sub>2</sub> process; TiO<sub>2</sub>/UV/H<sub>2</sub>O<sub>2</sub>, photocatalytic processes aided by H<sub>2</sub>O<sub>2</sub>; TiO<sub>2</sub>/UV/O<sub>3</sub>, photocatalytic processes aided by O<sub>3</sub>; TiO<sub>2</sub>/UV/O<sub>3</sub>/H<sub>2</sub>O<sub>2</sub>, photocatalytic processes aided by O<sub>3</sub>/H<sub>2</sub>O<sub>2</sub>; t-VOCs, total volatile organic compounds; UV, ultraviolet; VB, valence band; VNCs, volatile nitrogen compounds; VOCs, volatile organic compounds; VSCs, volatile sulfur compounds; WW, wastewater; ZnO, Zinc Oxide

\* Corresponding author.

E-mail address: [grzegorz.boczkaj@pg.edu.pl](mailto:grzegorz.boczkaj@pg.edu.pl) (G. Boczkaj).

<https://doi.org/10.1016/j.cej.2019.123488>

Received 22 July 2019; Received in revised form 28 October 2019; Accepted 11 November 2019

1385-8947/© 2019 The Authors. Published by Elsevier B.V. This is an open access article under the CC BY license (<http://creativecommons.org/licenses/by/4.0/>).

of chemicals achieving similar treatment efficiency when comparing with photolytic and non-catalytic technologies. The application of these technologies can be conducted in two alternative scenarios; whether to deplete the sulfides ions concentration or to maximize the treatment efficiency. In both options, the technologies studied are promising as a pre-treatment before other types of AOPs effective at neutral/acidic pH values or before a biological treatment stage. Further studies should be developed, by scaling up the process to a pilot scale in a real case scenario to check the possibility of its implementation in the industrial practice.

## 1. Introduction

Petroleum & Refinery effluents are known to contain several refractory and recalcitrant compounds, and a high load of organic pollutants, which can be difficult to treat effectively [1–4]. The available technologies used to treat such effluents include, electrocoagulation [5], coagulation–flocculation and flotation [6] catalytic vacuum distillation [7], activated sludge [8], activated carbon [9], Advanced Oxidation Processes (AOPs) [10] among others. There are some reviews concerning the treatment for this type of effluents, namely, catalytic [11], photocatalytic [12,13], membrane technology [14] and the combination of AOPs and biological technologies [15]. There are cases of petroleum & refinery wastewater (WW) that are generated at a strong alkaline pH, namely, spent caustic [16] and post-oxidative effluents from bitumen production [3]. In the case of post oxidative effluents from bitumen production, their caustic pH ( $\approx 11$ ), high concentration of sulfide ions present at the concentration level of 1–2 g/L and the presence of several types of volatile organic compounds (VOCs), limits the range of treatment technologies that can be applied, namely open air, biological and Fenton technologies. The VOCs present include many groups of compounds, i.e., oxygen volatile organic compounds (O-VOCs) (including phenol and its derivatives), volatile nitrogen compounds (VNCs) and volatile sulfur compounds (VSCs). These type of compounds were characterized in previous papers, where each group described was identified and quantified by dedicated method of detailed analysis [17–19]. The pH correction can lead to the generation of H<sub>2</sub>S (due to presence of sulfide ions) which must be avoided [20]. In addition, there is a risk of VOCs emission to the atmosphere if open air biological treatment technologies are used.

Recent studies described the treatment of post oxidative effluents using classic AOPs oxidants [21] and sulfate radical based AOPs oxidants [22], as technologies that obtained effective degradation of the VOCs and sulfide ions, along with the decrease in the pH to values close to neutral. In addition, they achieved partial chemical oxygen demand (COD) and biological oxygen demand (BOD<sub>5</sub>) reduction. These findings suggest that the technologies used are useful as a pre-treatment stage before biological treatment. Taking this into account and to attempt to improve the degradation of the organic load of the effluents (increase COD and BOD<sub>5</sub> reduction), the photolytic and photocatalytic processes were proposed and studied. In the case of the photocatalytic processes, the generation of reactive radicals, mostly as hydroxyl radicals (HO<sup>•</sup>), and their reaction with the compounds takes place on the surface of the catalyst, when properly activated by the ultraviolet (UV) light [23–27].

Some examples of catalysts include, Titanium Dioxide (TiO<sub>2</sub>), Zinc Oxide (ZnO) [28–30], or their doped materials like iron doped ZnO [31], iron doped TiO<sub>2</sub> [32], TiO<sub>2</sub> co-doped with two metallic compounds [33,34] or combined approaches such as ZnO immobilized on nanocellulose [35]. In addition, the use of a support can improve the surface area of the catalyst, decrease sintering, improve hydrophobicity and thermal hydrolytic, chemical stability and manage the reusability of the catalyst [36,37]. Cementitious nano TiO<sub>2</sub>-SiO<sub>2</sub> [38], glass–ceramic immobilized bismuth based catalysts [39,40], magnetic CuFe<sub>2</sub>O<sub>4</sub> nanoparticles [41], graphene oxide modified sea urchin-like  $\alpha$ -MnO<sub>2</sub> architectures [42], iron related nanostructures [43,44] are examples found in the literature that have been developed. Several reviews were performed to relate the state of the art of different types of catalysts. The application of graphene and carbon nanotubes was

reviewed using different configurations like doped and co-doped with several types of heteroatoms like O, S, F, P, B and N for the activation of peroxydisulfate and peroxymonosulfate [45]. A review in the different types of ZnO based catalysts in the treatment of various pollutants was performed. This work compared the efficiency of the solely use of ZnO in powder with ZnO doped with heteroatoms and transition metals and ZnO coupled with other semiconductor particles [46]. Also some reviews discussed the catalytic activity of TiO<sub>2</sub> in different configurations like simple powder, doped and co-doped with heteroatoms and transition metals, coupled with other semiconductors to evaluate the treatment efficiency of pollutants, toxins among others [47,48]. A structural design of the TiO<sub>2</sub> photocatalysis was also reviewed in several point of views to check the efficiency of the activation of the TiO<sub>2</sub> and its applications [49]. It is clear from these reviews that the mostly used and studied catalyst is TiO<sub>2</sub> due to its low cost and availability as well as chemical stability, nontoxicity, and high reactivity [50,51]. The photocatalytic and catalytic processes have been applied in several types of real effluents, seawater-soluble crude-oil fractions [52] petrochemical [53], petroleum & refinery [54–59] and post-treatment of refinery WW [60]. The common factor about these studies is that the effluents used had a relatively low organic load (COD between 100 and 200 mg/L) when comparing with the effluent used in this work, since some of them were collected after some treatment stages. In this work it is attempt to use photocatalytic AOPs in primary and highly polluted effluents before any treatment stage, so the challenge is more demanding.

Taking this into account, the goal of this work is to understand the synergy and the performance of the addition of the TiO<sub>2</sub> and UV to the classic AOPs based on external oxidants. A comparison between classic AOPs oxidants (O<sub>3</sub>, H<sub>2</sub>O<sub>2</sub>, O<sub>3</sub>/H<sub>2</sub>O<sub>2</sub>), photolytic AOPs (O<sub>3</sub>/UV, H<sub>2</sub>O<sub>2</sub>/UV, O<sub>3</sub>/H<sub>2</sub>O<sub>2</sub>/UV) and photocatalytic AOPs (TiO<sub>2</sub>/UV/O<sub>3</sub>, TiO<sub>2</sub>/UV/H<sub>2</sub>O<sub>2</sub>, TiO<sub>2</sub>/UV/O<sub>3</sub>/H<sub>2</sub>O<sub>2</sub>) was performed for treatment of the post-oxidative effluents from bitumen production at their natural conditions of their formation (no pH and temperature correction).

## 2. Materials and methods

### 2.1. Materials

Laboratory procedures were carried out using refinery post oxidative effluents from bitumen production plant from Lotos Asphalt (Grupa Lotos, Poland). The chemical characteristics are the following; COD within the range of 18–22 gO<sub>2</sub>/L, Biological Oxygen Demand after 5 days (BOD<sub>5</sub>) within the range of 5–6 gO<sub>2</sub>/L, Sulfides ions within the range of 1–2 g/L, pH 10.5–11, conductivity: 18,55 mS/cm.

H<sub>2</sub>O<sub>2</sub> (30%, v/v) was purchased from POCH Poland. The catalyst AEROXIDE® P25, titanium dioxide (TiO<sub>2</sub>) ( $\geq 99.5\%$  purity) was kindly given by Evonik Company. Antifoam agent, STRUKTOL SB 2032, was kindly provided by ICSO Chemical Production Polska

### 2.2. Apparatus

An acid-resistant steel closed cylindrical reactor with a total volume of 15 dm<sup>3</sup> was used for these studies and is illustrated in Fig. 1S in Supporting information (SI). It has 3 inlets, air, oxidant and WW inlet, and sample collection outlet. In the top of the reactor, one outlet for the exhaust air from the ozone technologies. To control the temperature the reactor was equipped with a temperature regulator model AR600

(APAR, Poland), coupled with a 2000 W heater. Detailed description of the reaction system is provided in SI section 1.1 and Fig. 1S. In the photolytic and photocatalytic processes, a medium pressure, mercury lamp model UVHQ 250Z (UV-technik, Germany) with a power of 250 W and a specific lamp power of 56 W/cm was used. This lamp was installed inside a chamber (marked as “b” symbol on Fig. 1S-I)–and is parallel to the vertical axis of the reactor. This chamber was connected to one of the windows of the reactor (number 5 in Fig. 1S-II). The WW was pumped into the reactor by a membrane (PTFE) pump model UGD 100/120-03 (Euralca, Italy). The recirculation of the effluent in the reactor through the UV chamber was obtained by means of a rotary vane pump model MS 632–4 B34 (Fluid-o-Tech, Italy). The ozone was fed by a Tytan 32 ozone generator having an efficiency of 70 mgO<sub>3</sub>/L of air. Air was used to produce ozone-H<sub>2</sub>O<sub>2</sub> was fed to the reactor using a Hitachi LaChrom HPLC Pump model L-7110. To perform the separation of the catalyst and the treated WW, an Heraeus Sepatech centrifuge was used.

The equipment used in the analysis of the volatile organic compounds was a Perkin Elmer Autosystem XL gas chromatograph (GC) with an autosampler, a flame photometric detector (FPD) (PerkinElmer, USA) to analyze the VSCs. To analyze the VNCs, a Perkin Elmer Autosystem XL gas chromatograph (GC) with an autosampler and nitrogen-phosphorus detector (NPD) (PerkinElmer, USA) was used. Analysis of the O-VOCs was performed using a HP 5890 II gas chromatograph coupled with a HP 5972A mass spectrometer (Hewlett-Packard, USA). Details of each procedure are fully described in our previous papers dedicated to each group of compounds [17–19]. COD determination was done using a HACH COD reactor and a HACH DR/2010 spectrophotometer. The oxygen concentration changes (before and after the 5-day incubation period of the BOD<sub>5</sub> method) were determined using an Elmetron COG-1 oxygen electrode connected to Elmetron CP-505. The reading in millivolts was recalculated to oxygen concentration on the basis of calibration curve. The samples during a 5 day period of incubation were stored in an incubation chamber (Flow Laboratories catalog number S1- 500–00). Sulfide concentration measurements were performed using an Elmetron EAg/S-01 sulfide/silver electrode in combination with an Elmetron RL-100 reference electrode (supporting electrolyte in the form of saturated solution of potassium chloride). The limit of detection of sulfide ions is 0.032 mg/L. The values in millivolts from the method to determine the sulfide ions were read by Elmetron CP-505 and recalculated to concentration of sulfide ions using calibration curve. pH was measured by Merck non-bleeding pH paper strips.

### 2.3. Effluent treatment

In every procedure, 5 dm<sup>3</sup> of effluent were added to the reactor. All procedures were done at original pH of the effluents without any adjustment, i.e. pH of 10.5–11, stirred at 200 rotations per minute (rpm) and heated until 40 °C (temperature which the effluents are generated). In the ozone and peroxide procedures, due to the high amount of foam produce from stirring and barbotage, a STRUKTOL SB 2032 antifoam agent, kindly provided by ICSO Chemical Production Polska, was used in the concentration of 200 ppm (selected during preliminary studies in this project). When the effluent reached the desired operational conditions, the catalyst was added by the upper part of the reactor and the recirculation pump was turned on. The catalyst was in contact with the effluent for 30 min before the beginning of the treatment. The oxidant dose was established depending on the molar ratio between the O<sub>2</sub> added from the oxidant source and the COD of the effluent (r<sub>ox</sub>). The method to determine the r<sub>ox</sub> is fully described in previous work [21]. The treatment time depended on the r<sub>ox</sub>. The pH was measured by non-bleeding pH strips in every sample taken. The temperature of the experiments did not change significant changes during the treatment time. Furthermore, the pressure of the treatment remained unchanged at 1 bar.

### 2.4. Process control

Samples with a total volume of 0.022 dm<sup>3</sup> were taken prior to catalyst addition and after the 30 min of contact to fully understand the adsorption phenomena by studying the changes in the concentration of the VOCs. After the treatment started, a samples of 0.022 dm<sup>3</sup> were taken every 15 min in the first hour of treatment, at 90 min, 120 min and every hour until the end of the treatment. The volume of collected samples were not significant in relation to the treated volume of effluent, thus it was not affecting the obtained results. The samples were afterwards centrifuged for 20 min at 5 000 rpm. Samples were collected with the purpose of analyzing the VOCs concentration, COD, BOD<sub>5</sub>, sulfide ions and pH. COD was measured using the Polish standard test method PN-ISO 15705:2005, based on the dichromate method by HACH. The BOD<sub>5</sub> was measured by the International Standard Norm 5815–1, where the samples were incubated at 20 ± 1 °C [21]. The method to determine the sulfide ions is detailed described in Section 1.2. of SI. The procedures to determine COD, BOD<sub>5</sub>, sulfide ions and pH were equal to our previous work and are described in detail elsewhere [22]. Regarding the volatile organic compounds monitoring, the sample preparation in all cases was done by dispersive liquid–liquid micro-extraction (DLLME). The obtained extracts were analyzed by means of

- gas chromatography with flame photometric detector (DLLME-GC-FPD) for VSCs [17]
- gas chromatography-mass spectrometry (DLLME-GC-MS) for O-VOCs [18]
- gas chromatography with nitrogen phosphorus detector (DLLME-GCNP) for VNCs [19].

The procedures are described in details in above referenced papers.

### 2.5. Quality assurance of the data

To assure the reproducibility and the reliability of the results shown, all procedures were done in triplicate. In addition, it was supported with the analysis of COD and BOD<sub>5</sub>, done also in triplicate for every sample, with a relative standard deviation (RSD) not higher than 2%.

## 3. Results and discussion

### 3.1. The role of UV and TiO<sub>2</sub> on the treatment effectiveness

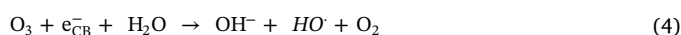
The literature regarding the AOPs clearly indicates that combination of UV with O<sub>3</sub>, or H<sub>2</sub>O<sub>2</sub> as well as O<sub>3</sub>/H<sub>2</sub>O<sub>2</sub> increases the yield of HO· available to react with the organic pollutants, increasing the treatment efficiency [50]. Furthermore, in the photocatalytic technologies, the TiO<sub>2</sub> is irradiated with enough energy, enabling an electron (e<sup>-</sup>) to be conducted from its valence band (VB) to the conductive band (CB), (bandgap energy). The outcoming of the irradiation is the formation of holes in the VB (h<sub>VB</sub><sup>+</sup>) that will act as oxidizing sites as described in Eq. (1) [61–63].

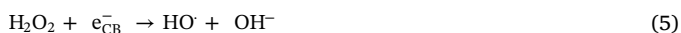


In the h<sub>VB</sub><sup>+</sup> of the TiO<sub>2</sub> surface, H<sub>2</sub>O and OH<sup>-</sup>, will act as electron donors, generating HO·, as demonstrated in Eqs. (2) and (3) [64].



If external oxidants are present in the medium like O<sub>3</sub> or H<sub>2</sub>O<sub>2</sub>, they will act as an e<sup>-</sup> acceptors, generating HO·, as described in Eqs. (4) and (5) [65–67].





Thus, to attempt to prove such mechanisms and statements, a comparison between classic AOPs oxidants ( $\text{O}_3$ ,  $\text{H}_2\text{O}_2$ ,  $\text{O}_3/\text{H}_2\text{O}_2$ ), photolytic AOPs ( $\text{O}_3/\text{UV}$ ,  $\text{H}_2\text{O}_2/\text{UV}$ ,  $\text{O}_3/\text{H}_2\text{O}_2/\text{UV}$ ) and photocatalytic AOPs ( $\text{TiO}_2/\text{UVO}_3$ ,  $\text{TiO}_2/\text{UV}/\text{H}_2\text{O}_2$ ,  $\text{TiO}_2/\text{UV}/\text{O}_3/\text{H}_2\text{O}_2$ ) was performed in bitumen effluents. In addition, the synergism of the combined photolytic and photocatalytic processes was studied to check the role of the UV and  $\text{TiO}_2$  addition to the classic AOPs oxidants.

### 3.1.1. COD reduction and VOCs degradation using classic AOPs oxidants, photolytic and photocatalytic processes

Fig. 1 depicts the COD reduction of the post oxidative effluents for the different advanced oxidation technologies. It is clear and proved that the sole use of  $\text{TiO}_2$  and UV were ineffective to degrade compounds present in such effluents. This is supported with the facts that the sole use of UV and  $\text{TiO}_2$  cannot generate  $\text{HO} \cdot$  in such conditions and also do not have oxidation potential to provide oxidation of the WW alone. The analysis of Fig. 1, also revealed that the photocatalytic processes without the addition of external oxidants,  $\text{TiO}_2/\text{UV}$  are also ineffective. It is proved that the generation of  $\text{HO} \cdot$  in the surface of the  $\text{TiO}_2$  particle, via Eqs. (2) and (3), is very poor and therefore providing no significant change in the primary COD. A possible explanation is related with the pH value and the point of zero charge (PZC) of the  $\text{TiO}_2$ . It is known that the PZC of the  $\text{TiO}_2$  is around 6.25 [13], which means that at the pH used the surface of the catalyst is negatively charged and the compounds present in the effluents (having mainly neutral character) have repulsive attraction to the negative charge of the surface. A second explanation to this phenomenon can be related with the presence of carbonates and other scavengers that react with the  $\text{HO} \cdot$  instead of the organic pollutants present in the WW:

Fig. 1 and Table 2 also revealed that the photolytic processes obtained higher treatment efficiency for all oxidants studied comparing to the sole oxidant processes. When the  $\text{TiO}_2$  was added to the photolytic processes, i.e.,  $\text{H}_2\text{O}_2/\text{UV}$ ,  $\text{O}_3/\text{UV}$  and  $\text{O}_3/\text{H}_2\text{O}_2/\text{UV}$  some differences were observed. The addition of the  $\text{TiO}_2$  to the  $\text{O}_3/\text{UV}$  and  $\text{O}_3/\text{H}_2\text{O}_2/\text{UV}$  processes had a minor positive influence on the COD reduction. In the case of the  $\text{TiO}_2/\text{UV}/\text{O}_3/\text{H}_2\text{O}_2$  the rate of degradation was significantly higher in the first 60 min. The most interesting result relates to the fact that  $\text{H}_2\text{O}_2/\text{UV}$  process had a higher COD reduction than  $\text{TiO}_2/\text{UV}/\text{H}_2\text{O}_2$ , 31% and 24% respectively. It seems that the addition of  $\text{TiO}_2$  inhibit the reduction of the organic load of the effluent. A possible hypothesis is related to the increase of turbidity caused by addition of the  $\text{TiO}_2$ , which decreases the  $\text{H}_2\text{O}_2$  activation. The turbidity increase is inhibiting the  $\text{H}_2\text{O}_2$  conversion by UV, and the predominant reaction is the  $\text{H}_2\text{O}_2$  at basic pH which led to formation of less reactive species

than hydroxyl radicals, which results in the decrease of effectiveness observed. Other hypothesis is related with a different degradation pathway of the compounds via photocatalytic process using  $\text{TiO}_2$  and  $\text{H}_2\text{O}_2$ , in which the by-products are not further degraded in a specific step.

To obtain a more solid opinion of the role of the  $\text{TiO}_2$  and UV in the treatment behavior of the bitumen effluents, the degradation of the VOCs detected were analyzed. In order to determine whether the VOCs are degraded and not emitted when using  $\text{O}_3$  related technologies, the phenomena of partial stripping of the VOCs was studied, due to the significant gas barbotage in these technologies. The preliminary studies passed through the effluents nitrogen gas solely (instead of air to insure that no oxidation by oxygen takes place) at the highest flowrate used in this work during 440 min. The VOCs with boiling point up to  $100^\circ\text{C}$  were removed by nitrogen barbotage in less than 30% and less than 10% in the case of the VOCs with boiling point above  $150^\circ\text{C}$ . The effluents studied are collected prior to the biological stage in the WWTP and the goal is to degrade the VOCs content. Thus, this effect is positive, since, even if a small amount of the VOCs were removed by gas stripping, it is a common practice in the industry to use a thermal treatment of gases prior to its emission to atmosphere (i.e., they are used to supply flame towers, burners etc.), which convert VOCs to nontoxic carbon dioxide. That is why this effect is positive in terms of the goal of this paper.

In respect to the VOCs monitoring, Fig. 2 and Table 1S, 2S and 3S present an overview of the oxygen volatile organic compounds (O-VOCs), volatile nitrogen compounds (VNCs) and volatile sulfur compounds (VSCs) and total-VOCs (t-VOCs) degradation in the different technologies. It is clear that the t-VOCs degradation increased when  $\text{H}_2\text{O}_2$  was activated by UV or  $\text{TiO}_2/\text{UV}$  system. Also in O-VOCs and VNCs the increase is significant. Thus, the decrease of the COD reduction in the  $\text{H}_2\text{O}_2$  related AOPs is not related with the lower degradation of the VOCs. Fig. 2S and 3S in SI revealed that p-toluidine, and phenolic compounds reported higher degradation. Looking to their structure,  $\text{HO} \cdot$  will react with the compounds promoting the addition of OH group to ring and afterwards the cleavage of the ring to carboxylic acids, which seems to not contribute to an increase of the COD. Thus, a possible explanation can be related with the fact that some of the compounds not detected by the used method (i.e. not oxidized under COD measurement conditions) are converted to by-products that can contribute to a higher COD (i.e. these compounds start to be available for oxidation during COD measurement). Regarding the  $\text{O}_3$  related processes, similar t-VOCs degradation was reported, with approx. 80% degradation of t-VOCs in  $\text{O}_3$ ,  $\text{O}_3/\text{UV}$  and  $\text{TiO}_2/\text{UV}/\text{O}_3$  processes. In  $\text{TiO}_2/\text{UV}/\text{O}_3$  processes VNCs and VSCs were fully degraded and exhibit a higher degradation rate comparing to  $\text{O}_3$  and  $\text{O}_3/\text{UV}$ . In the O-VOCs

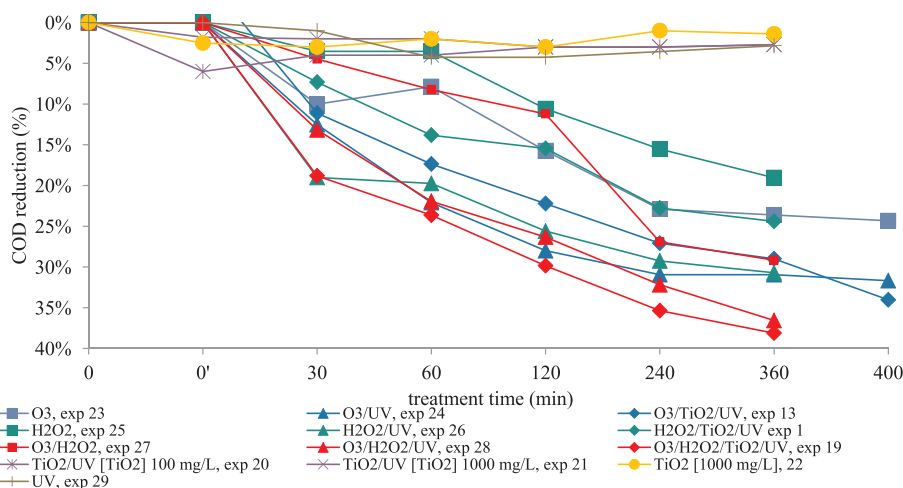


Fig. 1. COD reduction profile during treatment time of different AOPs studied.

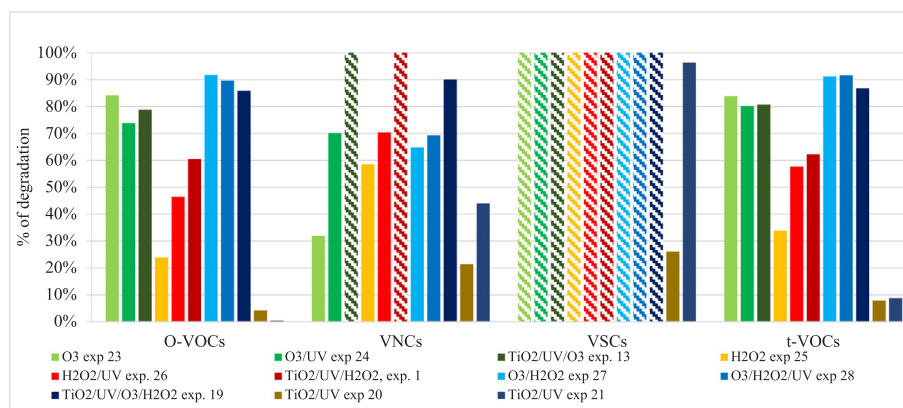


Fig. 2. t-VOCs, O-VOCs, VSCs, VNCs degradation after treatment time of different AOPs.

the degradation rate was similar. In the  $O_3/H_2O_2$  related processes a significant difference was observed, where  $O_3/H_2O_2/UV$  obtained 90% of t-VOCs degradation while  $TiO_2/UV/O_3/H_2O_2$  achieved 84%. This difference is mainly due to the degradation of 1-propanol (Fig. 3S), which was significantly lower in  $TiO_2/UV/O_3/H_2O_2$  than in the non-catalytic processes decreasing the O-VOCs degradation from 87% ( $O_3/H_2O_2/UV$ ) to 83% ( $TiO_2/UV/O_3/H_2O_2$ ). In the VNCs, the opposite result was obtained, where the addition of UV to  $O_3/H_2O_2$  and  $TiO_2$  to  $O_3/H_2O_2/UV$  increased their degradation significantly. VSCs were effectively degraded, with concentrations after treatment below the limit of detection (LOD) in all processes.

### 3.1.2. Synergism of the combined photolytic and photocatalytic processes

The synergism effect of the combined processes was evaluated using the COD reduction of the processes studied. The synergism of the photolytic and photocatalytic combined processes was calculated by the Eqs. (6) and (7) below respectively.

$$S_1 = \frac{COD_{reduction}(UV - Oxidant)}{COD_{reduction}(UV) + COD_{reduction}(Oxidant)} \quad (6)$$

$$S_2 = \frac{COD_{reduction}(Oxidant - UV - Catalyst)}{COD_{reduction}(oxidant) + COD_{reduction}(UV) + COD_{reduction}(catalyst)} \quad (7)$$

This was calculated for the  $H_2O_2$ ,  $O_3$  and  $O_3/H_2O_2$  oxidants. The higher the value of  $S_1$  and  $S_2$ , the higher the synergism of the combined process. A significant synergism was observed in photolytic processes using  $H_2O_2$  ( $S_1$ , 1.19),  $O_3$  ( $S_1$ , 1.23) and  $O_3/H_2O_2$  ( $S_1$ , 1.06). As explained in section 3.1., the combination of UV with these oxidants increased significantly the generation of  $HO^\cdot$  and consequently increase

its degradation efficiency, which can explain the high values of synergy.  $O_3/UV$  had the highest synergism, probably due to ability to generate  $HO^\cdot$  from  $O_3$  at basic pH. The synergism maintained the same level when  $TiO_2$  and UV was combined with  $O_3$  ( $S_2$  1.22) and increased for  $O_3/H_2O_2$  ( $S_2$  1.15 for photocatalytic process vs 1.06 for photolytic process). In contrast, the synergism slightly decreased when  $TiO_2$  and UV were combined with  $H_2O_2$  ( $S_2$  1.06). This decrease can be explained by the lack of efficacy of  $TiO_2$  and UV to react with  $H_2O_2$  and between them, probably due to high turbidity or even with the dissociation of  $H_2O_2$  at basic pH to less reactive species before the reaction with UV or  $TiO_2$ . Nevertheless, all the combined processes obtained a positive synergism values ( $S$  values above 1), which is a positive outcome of this work. Thus, the addition of  $TiO_2$  to the photolytic processes had a positive synergistic effect in the treatment efficiency of the bitumen effluents. A positive synergism can obtain the same level of COD reduction needing less treatment time, which can influence the cost of treatment that will be discussed in a further section.

### 3.2. Photocatalytic processes using external oxidants

To analyze the photocatalytic processes aided with external classic AOPs oxidants in detail using the post oxidative effluents, water quality parameters like, COD,  $BOD_5$ , biodegradability, sulfide ions and VOCs content were monitored before, during and after treatment. Operational parameters like  $r_{ox}$  and catalyst concentration were studied to reach the highest degradation possible using the less amount of oxidants and catalyst possible at an economic cost.

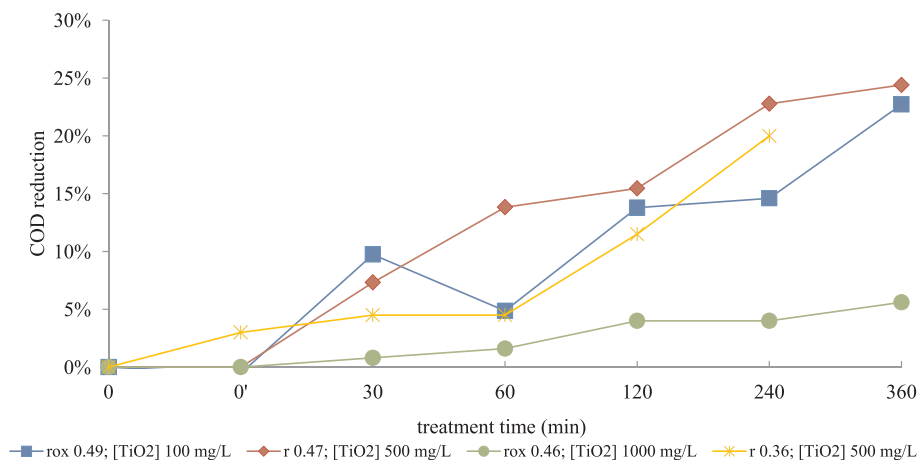


Fig. 3. COD reduction profile during treatment time of  $TiO_2/UV/H_2O_2$  processes.

### 3.2.1. Photocatalytic process using $\text{TiO}_2$ assisted with $\text{H}_2\text{O}_2$

Fig. 3 and Table 2 depicts the COD reduction of the post oxidative effluents under different catalyst concentration and  $r_{\text{ox}}$  values. It is clear that the  $r_{\text{ox}}$  plays a critical role in the effectiveness of the treatment used, with a significant decrease in the COD reduction when the  $r_{\text{ox}}$  was decreased. Regarding the influence of the  $\text{TiO}_2$ , there is an optimal catalyst concentration in which the COD reduction is the highest. At 500 mg/L of  $\text{TiO}_2$  the COD reduction achieved 24%, a further increase to 1000 mg/L had a significant negative impact on the COD reduction, with only 6% of COD reduction. Regarding the  $\text{BOD}_5$  parameter a different profile was obtained (Table 2). For less efficient COD reduction processes, the  $\text{BOD}_5$  reduction was significantly higher. A possible explanation for such behavior can be related with the higher capability of the technology to degrade compounds that can be degraded by the biological approach than the non-biodegradable compounds. In addition, the lower yield of radicals generation can also be related with such behavior. The optimal process for total organic load reduction of the effluents was experiment 1 from Table 1 ( $r_{\text{ox}}$  of 0.49; 100 mg/L of  $\text{TiO}_2$ ) achieving 23% and 53% of COD and  $\text{BOD}_5$  reduction respectively.

Fig. 4 reveals the t-VOCs, O-VOCs, VNCs and VSCs reduction in the most effective COD reduction processes studied. VNCs and VSCs were degraded to a level below the LOD values of the analytical methods (generally very sensitive methods, thus the obtained results can be discussed in terms of complete removal) in processes using similar  $r_{\text{ox}}$  (0.47 and 0.49) using 100 and 500 mg/L of  $\text{TiO}_2$  respectively. In the case of O-VOCs they achieved partial degradation. The process using 500 mg/L of  $\text{TiO}_2$  achieved slightly higher reduction than the process using  $[\text{TiO}_2]$  of 100 mg/L, 61 comparing to 55% respectively, which can be explained by the increase in the degradation rate via AOP. Specific compounds like furfural, cyclohexanol and cyclohexanone had

their concentration increased after treatment applying a  $r_{\text{ox}}$  of 0.49 and 100 mg/L of  $\text{TiO}_2$ . This is probably due to their generation from the oxidation of other compounds via AOP. Similar behavior was found previous studied using  $\text{H}_2\text{O}_2$  related processes [21]. The optimal process to degrade VOCs was experiment 1 ( $r_{\text{ox}}$  of 0.49; 100 mg/L of  $\text{TiO}_2$ ), with 58% of t-VOCs degradation, same process in the case of the COD and  $\text{BOD}_5$  reduction.

### 3.2.2. Photocatalytic process using $\text{TiO}_2$ assisted with $\text{O}_3$

Fig. 5 presents the COD reduction over treatment time using  $\text{TiO}_2/\text{UV}/\text{O}_3$  with different catalyst concentration and  $r_{\text{ox}}$  values. Fig. 5, depicts a minor influence of the  $\text{TiO}_2$  concentration on the COD reduction keeping similar  $r_{\text{ox}}$  value  $0.43 \pm 0.02$ . In the  $\text{BOD}_5$  reduction only at 2000 mg/L of  $\text{TiO}_2$  there was a significant  $\text{BOD}_5$  reduction from 40 to 57%, comparing with 100 and 500 mg/L of  $\text{TiO}_2$ . Apparently, the increase concentration of  $\text{TiO}_2$  in the medium is producing reactive species that are degrading the biological degradable compounds, contributing to the  $\text{BOD}_5$  significant decrease. A possible hypothesis for such behavior can be related with the point of zero charge (PZC) and the pH of effluent was already explained in section 3.1. Such behavior was reported in our previous work using photocatalytic assisted with  $\text{O}_3$  [68]. Once more, Fig. 5 and Table 2 once more reveals that the  $r_{\text{ox}}$  value is crucial for an effective COD and  $\text{BOD}_5$  reduction. It is clear that for low  $r_{\text{ox}}$ , 0.11 and 0.27 the treatment efficiency was proportional to oxidant dose with 14 and 25% of COD reduction. It means that almost total dose of the oxidant was utilized for COD lowering predicted via AOPs chemistry. But when the  $r_{\text{ox}}$  value was increased twice, to 0.56, the COD reduction did not increase twice and reached 34%. This means that the oxidant utilization effectiveness decreased and only a part of the oxidant added was used for COD lowering comparing to the

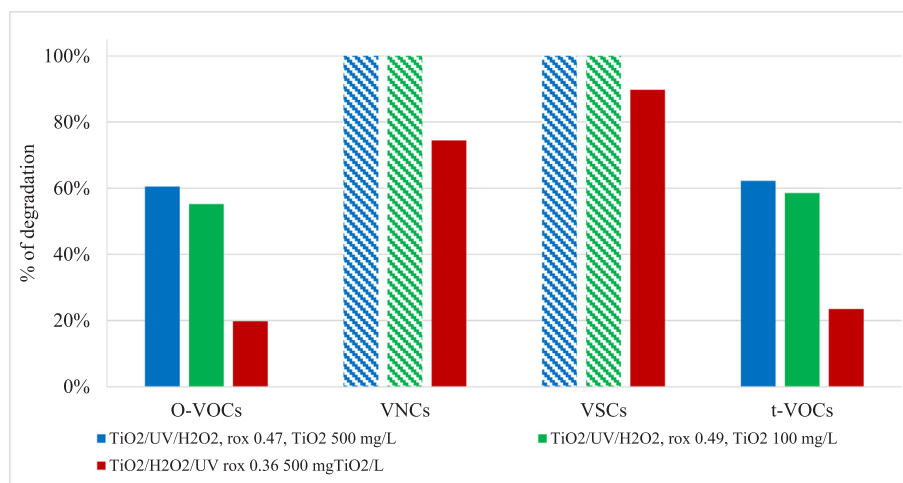
**Table 1**  
Operational parameters of the non-catalytic, photolytic and photocatalytic AOPs studied.

No.	Process	$r_{\text{ox}}$	Treatment time (min)	Oxidant amount (g)	$\text{TiO}_2$ (mg/L)	Oxidant Flowrate (ml/min)	$[\text{O}_3]$ (mg/L)	Air flowrate (L/min)	ratio of $\text{O}_3/\text{H}_2\text{O}_2$
1	$\text{TiO}_2/\text{H}_2\text{O}_2/\text{UV}$	0.49	274	47.81	100	0.529	–	–	–
2	$\text{TiO}_2/\text{H}_2\text{O}_2/\text{UV}$	0.47	274	47.81	500	0.529	–	–	–
3	$\text{TiO}_2/\text{H}_2\text{O}_2/\text{UV}$	0.46	274	47.81	1000	0.529	–	–	–
4	$\text{TiO}_2/\text{H}_2\text{O}_2/\text{UV}$	0.38	240	55.78	500	0.704	–	–	–
5	$\text{TiO}_2/\text{H}_2\text{O}_2/\text{UV}$	0.07	240	11.16	500	0.141	–	–	–
6	$\text{TiO}_2/\text{H}_2\text{O}_2/\text{UV}$	0.19	240	27.89	500	0.352	–	–	–
25	$\text{H}_2\text{O}_2$	0.55	274	58.44	–	0.647	–	–	–
26	$\text{H}_2\text{O}_2/\text{UV}$	0.56	274	58.44	–	0.647	–	–	–
7	$\text{TiO}_2/\text{O}_3/\text{UV}$	0.45	274	56.25	100	–	10.3	20	–
8	$\text{TiO}_2/\text{O}_3/\text{UV}$	0.43	274	56.25	500	–	10.3	20	–
9	$\text{TiO}_2/\text{O}_3/\text{UV}$	0.43	274	56.25	1000	–	10.3	20	–
10	$\text{TiO}_2/\text{O}_3/\text{UV}$	0.41	274	56.25	2000	–	10.3	20	–
11	$\text{TiO}_2/\text{O}_3/\text{UV}$	0.12	260	16.5	500	–	12.5	5	–
12	$\text{TiO}_2/\text{O}_3/\text{UV}$	0.27	260	41.25	500	–	10.6	15	–
13	$\text{TiO}_2/\text{O}_3/\text{UV}$	0.56	400	82.5	500	–	10.3	20	–
23	$\text{O}_3$	0.56	400	82.5	–	–	10.3	20	–
24	$\text{O}_3/\text{UV}$	0.57	400	82.5	–	–	10.3	20	–
14	$\text{TiO}_2/\text{O}_3/\text{H}_2\text{O}_2/\text{UV}$	0.52	360	96.03	100	0.187	10.3	20	0.3
15	$\text{TiO}_2/\text{O}_3/\text{H}_2\text{O}_2/\text{UV}$	0.61	360	96.03	1000	0.187	10.3	20	0.3
16	$\text{TiO}_2/\text{O}_3/\text{H}_2\text{O}_2/\text{UV}$	0.33	360	70.45	1000	0.146	10.7	15	0.3
17	$\text{TiO}_2/\text{O}_3/\text{H}_2\text{O}_2/\text{UV}$	0.54	440	117.12	500	0.187	10.3	20	0.3
18	$\text{TiO}_2/\text{O}_3/\text{H}_2\text{O}_2/\text{UV}$	0.13	290	23.48	500	0.1	12.5	5	0.3
19	$\text{TiO}_2/\text{O}_3/\text{H}_2\text{O}_2/\text{UV}$	0.28	280	58.71	500	0.146	10.6	15	0.3
27	$\text{O}_3/\text{H}_2\text{O}_2$	0.3	280	58.7	–	0.146	10.7	15	0.3
28	$\text{O}_3/\text{H}_2\text{O}_2/\text{UV}$	0.28	280	58.7	–	0.146	10.7	15	0.3
20	$\text{TiO}_2/\text{UV}$	–	360	–	100	–	–	–	–
21	$\text{TiO}_2/\text{UV}$	–	360	–	1000	–	–	–	–
29	UV	–	400	–	–	–	–	–	–
22	$\text{TiO}_2$	–	360	–	1000	–	–	–	–

**Table 2**

Main results of the non-catalytic, photolytic and photocatalytic processes studied.

No.	Process	$r_{ox}$	COD reduction (%)	BOD <sub>5</sub> reduction (%)	Final pH	Sulfide ions reduction (%)	Biodegradability 0	Biodegradability f
1	TiO <sub>2</sub> /H <sub>2</sub> O <sub>2</sub> /UV	0.49	23	53	9.75	100.0	0.23	0.14
2	TiO <sub>2</sub> /H <sub>2</sub> O <sub>2</sub> /UV	0.47	24	26	10.5	99.4	0.22	0.21
3	TiO <sub>2</sub> /H <sub>2</sub> O <sub>2</sub> /UV	0.46	6	57	10.5	100.0	0.39	0.18
4	TiO <sub>2</sub> /H <sub>2</sub> O <sub>2</sub> /UV	0.38	20	–	10.5	62.2	–	–
5	TiO <sub>2</sub> /H <sub>2</sub> O <sub>2</sub> /UV	0.07	3	–	11	–	–	–
6	TiO <sub>2</sub> /H <sub>2</sub> O <sub>2</sub> /UV	0.19	8	–	11	–	–	–
25	H <sub>2</sub> O <sub>2</sub>	0.55	18	32	11	99.4	0.28	0.24
26	H <sub>2</sub> O <sub>2</sub> /UV	0.56	25	46	11	100	0.35	0.28
7	TiO <sub>2</sub> /O <sub>3</sub> /UV	0.45	31	40	9	99.9	0.43	0.38
8	TiO <sub>2</sub> /O <sub>3</sub> /UV	0.43	33	41	9.25	100.0	0.42	0.36
9	TiO <sub>2</sub> /O <sub>3</sub> /UV	0.43	28	33	9	99.9	0.41	0.38
10	TiO <sub>2</sub> /O <sub>3</sub> /UV	0.41	33	57	9.5	100.0	0.41	0.26
11	TiO <sub>2</sub> /O <sub>3</sub> /UV	0.12	12	26	10	99.5	0.36	0.33
12	TiO <sub>2</sub> /O <sub>3</sub> /UV	0.27	25	33	10	100.0	0.37	0.32
13	TiO <sub>2</sub> /O <sub>3</sub> /UV	0.56	34	31	9.5	99.8	0.36	0.36
23	O <sub>3</sub>	0.56	23	18	9.5	100	0.27	0.28
24	O <sub>3</sub> /UV	0.57	32	38	9.5	99.4	0.32	0.26
14	TiO <sub>2</sub> /O <sub>3</sub> /H <sub>2</sub> O <sub>2</sub> /UV	0.52	21	6	9	98.8	0.28	0.37
15	TiO <sub>2</sub> /O <sub>3</sub> /H <sub>2</sub> O <sub>2</sub> /UV	0.61	45	66	9	99.7	0.34	0.21
16	TiO <sub>2</sub> /O <sub>3</sub> /H <sub>2</sub> O <sub>2</sub> /UV	0.33	34	–	9.5	100	–	–
17	TiO <sub>2</sub> /O <sub>3</sub> /H <sub>2</sub> O <sub>2</sub> /UV	0.54	28	33	9.5	99.8	0.33	0.34
18	TiO <sub>2</sub> /O <sub>3</sub> /H <sub>2</sub> O <sub>2</sub> /UV	0.13	27	45	10	99.5	0.35	0.33
19	TiO <sub>2</sub> /O <sub>3</sub> /H <sub>2</sub> O <sub>2</sub> /UV	0.28	38	32	9.75	99.6	0.32	0.35
27	O <sub>3</sub> /H <sub>2</sub> O <sub>2</sub>	0.3	29	49	9.5	98.2	0.35	0.28
28	O <sub>3</sub> /H <sub>2</sub> O <sub>2</sub> /UV	0.28	34	39	9.75	100	0.33	0.31
20	TiO <sub>2</sub> /UV	–	3	–	11	–	–	–
29	UV	–	3	–5	11	–	0.32	0.36

**Fig. 4.** t-VOCs, O-VOCs, VSCs, VNCs degradation after treatment in the TiO<sub>2</sub>/UV/H<sub>2</sub>O<sub>2</sub> processes.

predicted value. Some amount of the oxidant was either dissociated to other less reactive radicals or compounds, which did not react with the organic compounds present. In terms of BOD<sub>5</sub>, the  $r_{ox}$  value had a moderate influence on lowering of this parameter. The increase of 0.11 to 0.27 in the  $r_{ox}$  value did not significantly increase the BOD<sub>5</sub> reduction, just from 26 to 33% respectively. The influence became slightly negative from 0.27 to 0.56 with a decrease of 2% in the BOD<sub>5</sub> reduction (33 to 31% respectively). Thus, the optimal TiO<sub>2</sub>/UV/O<sub>3</sub> processes to degrade the COD and BOD<sub>5</sub> from the bitumen effluents was experiment 8 ( $r_{ox}$  0.43; 500 mg/L of TiO<sub>2</sub>) with 33 and 41% of COD and BOD<sub>5</sub> reduction.

Fig. 6 shows the t-VOCs, O-VOCs, VNCs and VSCs degradation in the most effective processes of TiO<sub>2</sub>/UV/O<sub>3</sub>. It is clear that they were effective in degrading VNCs and VSCs monitored, reaching full degradation in all processes. Only the process TiO<sub>2</sub>/UV/O<sub>3</sub> using a  $r_{ox}$  of 0.43 and 500 mg/L of TiO<sub>2</sub> was able to degrade completely all O-VOCs. The critical compounds which were responsible for a VOCs degradation decrease when the  $r_{ox}$  changed were non-aromatic compounds, i.e., 1-

propanol, furfural, cyclohexanol and cyclohexanone (Fig. 4S). In addition, it is possible to observe in Fig. 4S that 1-propanol and furfural had their concentration increase after treatment in processes using 0.11 and 0.27  $r_{ox}$  value at 500 mg/L of TiO<sub>2</sub>. This can be related with their generation from oxidation of other compounds present in the effluents. This phenomenon or mechanism was also revealed in previous works using same oxidants and effluent [21,22]. Thus looking into the t-VOCs in Fig. 6 it is clear that the optimal process to degrade effectively the VOCs monitored was the same to degrade COD and BOD<sub>5</sub>, was experiment 8 ( $r_{ox}$  0.43; 500 mg/L of TiO<sub>2</sub>) with at least 97% of t-VOCs degradation.

It is clear that TiO<sub>2</sub>/UV/O<sub>3</sub> reach a higher treatment efficiency than TiO<sub>2</sub>/UV/H<sub>2</sub>O<sub>2</sub>, due to higher VOCs degradation and COD reduction and using less amount of oxidants. This can be related with the higher yield of HO· generation using O<sub>3</sub> rather than H<sub>2</sub>O<sub>2</sub>, with the higher oxidation potential of O<sub>3</sub> comparing with H<sub>2</sub>O<sub>2</sub> and due to the pH of the medium, alkaline, which favors the HO· generation using O<sub>3</sub>.

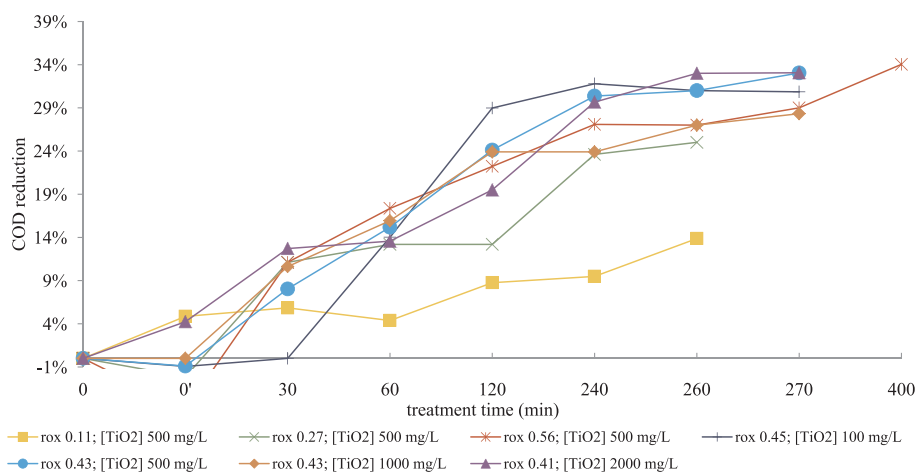


Fig. 5. COD reduction profile during treatment time of  $\text{TiO}_2/\text{UV}/\text{O}_3$  processes.

### 3.2.3. Photocatalytic process using $\text{TiO}_2$ assisted with $\text{O}_3/\text{H}_2\text{O}_2$

Section 3.1. revealed that  $\text{TiO}_2/\text{UV}/\text{O}_3/\text{H}_2\text{O}_2$  processes were the most effective to degrade the bitumen effluents and that further studies should be performed. Fig. 7 and Table 2 revealed the COD and  $\text{BOD}_5$  reduction during treatment time on  $\text{TiO}_2/\text{UV}/\text{O}_3/\text{H}_2\text{O}_2$  using different catalyst concentration and  $r_{\text{ox}}$  values. Keeping the  $r_{\text{ox}}$  constant ( $0.53 \pm 0.01$ ), the catalyst concentration had a minor significance on the COD reduction with an increase of 5% of COD reduction (from 29 to 34%) when increasing from 100 to 500 mg/L of  $\text{TiO}_2$ . Keeping constant another  $r_{\text{ox}}$  value ( $0.30 \pm 0.02$ ) varying the  $\text{TiO}_2$  concentration from 500 to 1000 mg/L there was a decrease from 38 to 34% respectively. A possible explanation for such results was explained in the section 3.1 and it is related with the PCZ of  $\text{TiO}_2$  and the pH of the WW. In contrast, keeping the concentration of  $\text{TiO}_2$  in 500 mg/L, it was clear that the  $r_{\text{ox}}$  had a significant effect on the treatment efficiency at a  $r_{\text{ox}}$  of 0.13 the COD and  $\text{BOD}_5$  reduction was 28 and 33% respectively and when a  $r_{\text{ox}}$  of 0.28 was applied it reach 38 and 32% of COD and  $\text{BOD}_5$  reduction respectively. It reveals that all the theoretical amount of oxidant added to degrade 13 and 28% of the COD of the effluent could actually degrade 28 and 38% respectively. It exceeded approx. 100% and 30% the COD reduction theoretical value, proving the important role of the  $\text{TiO}_2$  addition to the combination of UV with peroxone. Nevertheless, doubling the  $r_{\text{ox}}$  value (0.54) did not contribute to a higher degradation, by the contrary it contributed to a decrease of 4%, from 38 to 34% in the COD reduction. Also the  $r_{\text{ox}}$  value had a significant impact when the catalyst concentration was kept at 1000 mg/L. The decrease of the  $r_{\text{ox}}$

from 0.61 to 0.33 decreased the COD reduction from 45 to 34%. In overall, looking to the COD reduction, the best processes used a  $r_{\text{ox}}$  of 0.61 and 1000 mg/L of  $\text{TiO}_2$ . Nevertheless, the optimal process in terms of COD and  $\text{BOD}_5$  reduction was experiment 19 ( $r_{\text{ox}}$  0.28; 500 mg/L of  $\text{TiO}_2$ ) with 38 and 32% of COD and  $\text{BOD}_5$  reduction respectively. This process proved the usefulness of photocatalytic process, i.e. obtained COD reduction is much higher than the expected one on the basis of added amount of oxidant.

A monitoring of the VOCs present in the effluents of the  $\text{TiO}_2/\text{UV}/\text{O}_3/\text{H}_2\text{O}_2$  processes was conducted. Fig. 8 depicts the t-VOCs, O-VOCs, VNCs and VSCs degradation in the  $\text{TiO}_2/\text{UV}/\text{O}_3/\text{H}_2\text{O}_2$  processes. VNCs and VSCs were completely degraded after treatment in all processes studied with exception of VNCs in the process using a  $r_{\text{ox}}$  of 0.33 and 1000 mg/L of  $\text{TiO}_2$ . Regarding the O-VOCs, the scenario changed. Only processes using a  $r_{\text{ox}}$  of 0.52 and 100 mg/L of  $\text{TiO}_2$  and 0.61 and 1000 mg/L of  $\text{TiO}_2$  completely degraded all the O-VOCs. In the processes that kept constant the concentration of 500 mg/L of  $\text{TiO}_2$  the degradation was not so effective. The compounds responsible for such behavior were 1-propanol, furfural and cyclohexanol as exhibited in Fig. 5S. In the case of 1-propanol in experiment 17 and furfural in experiment 18 the concentration after treatment increased, influencing the overall degradation of the t-VOCs. Such behavior can be related with the formation of these compounds as the result of the oxidation/degradation of other compounds present in the effluents. In overall the optimal process to degrade the VOCs using  $\text{TiO}_2/\text{UV}/\text{O}_3/\text{H}_2\text{O}_2$  was experiment 14 ( $r_{\text{ox}}$  0.52; 100 mg/L of  $\text{TiO}_2$ ) with all compounds

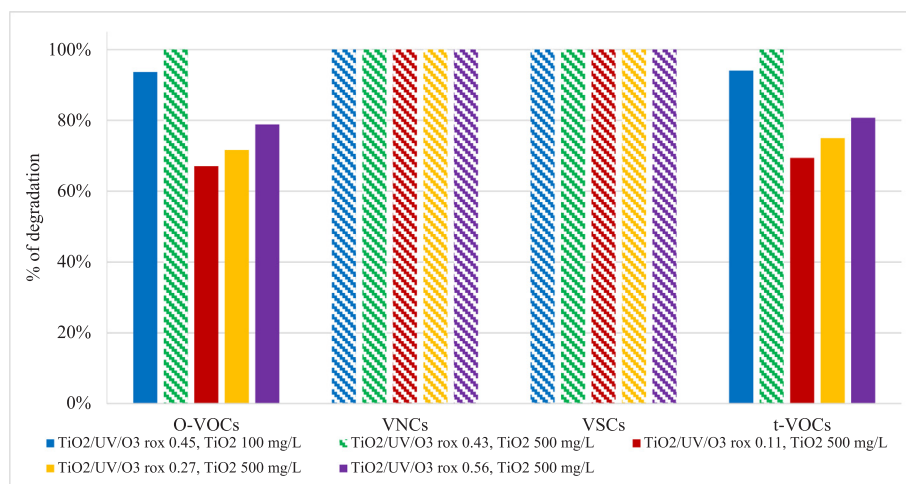


Fig. 6. t-VOCs, O-VOCs, VSCs, VNCs degradation after treatment in the  $\text{TiO}_2/\text{UV}/\text{O}_3$  processes.



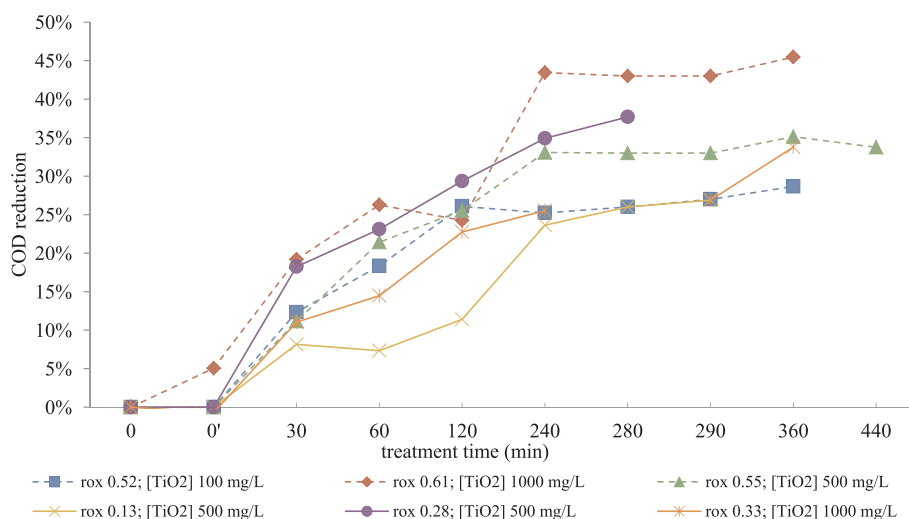


Fig. 7. COD reduction profile during treatment time of.  $\text{TiO}_2/\text{UV}/\text{O}_3/\text{H}_2\text{O}_2$  processes.

monitored and compared reached complete degradation.

Comparing  $\text{TiO}_2/\text{UV}/\text{O}_3/\text{H}_2\text{O}_2$  with  $\text{TiO}_2/\text{UV}/\text{O}_3$ , it reveals higher COD reduction using a lower  $r_{ox}$  value (38 comparing with 33% COD reduction) and the same  $\text{TiO}_2$  concentration. In contrast, it reached 84% t-VOCs degradation and 32% of  $\text{BOD}_5$  reduction, lower than  $\text{TiO}_2/\text{UV}/\text{O}_3$  (97% t-VOC degradation and 41%  $\text{BOD}_5$  reduction). Thus, a cost evaluation is mandatory to understand which technology is more promising.

### 3.3. Comparison of degradation effectiveness between model and real effluents

To study the effect of the water matrix, the VOCs degradation was studied and compared in the real effluents and model WW. 8 VOCs studied in this work were also studied in the previous work using a model WW [68]. Table 4S presents the degradation of the 8 VOCs in the model and real WW and Table 5S their respective reaction rate constant (k).

Analyzing the Table 4S, the furfural degradation decreases when changing from a model to a real WW matrix. However, some interesting behavior in the concentration profile during degradation was observed. The degradation increases for some time during the treatment and in the final stage of treatment it decreases again in all processes studied with exception of  $\text{H}_2\text{O}_2$ , where the concentration increased constantly during the treatment time. This sustains the theory that this compound

is a by-product of the degradation of other compounds not present in the model WW. Another interesting fact was observed in case of 2-nitrophenol. This compound had its concentration increased for the  $\text{H}_2\text{O}_2$  and  $\text{H}_2\text{O}_2/\text{UV}$  using model WW, while in the real effluents the opposite occurred. In addition, the  $\text{O}_3/\text{H}_2\text{O}_2$  related processes, its degradation was lower in model WW than in real effluents. A possible hypothesis for such behavior can be related with specific compounds present in the model WW and not present in the real effluents which can generate 2-nitrophenol as a by-product. Other hypothesis is based on comparison of the phenol and benzene degradation profile. Its concentration increased during the treatment time only in the  $\text{H}_2\text{O}_2$  and  $\text{H}_2\text{O}_2/\text{UV}$  processes using model WW. During this time, the increased concentration of these compounds can react with nitrite and nitrate ions, generated by  $\text{N}_2$ , to produce 2-nitrophenol, rather than reacting with  $\text{HO}^\cdot$ . These radicals are present in a lower amount, due to the fact that the  $\text{H}_2\text{O}_2$  at basic pH produces less powerful reactive species

In overall a decrease in the VOCs degradation in the real effluents was observed comparing with model WW in the  $\text{H}_2\text{O}_2$  related processes. On the other processes, no significant differences were observed. Nevertheless, the k values decrease for all compounds in case of real effluents treatment comparing with the model WW as observed in Table 5S. A possible explanation for such findings can be related with the water matrix of the real effluents. The turbidity value measured for these effluents is 41, 6 NTU, which indicates high primary turbidity of the effluent. Addition of even small amounts of  $\text{TiO}_2$  (such as 5 mg/L)

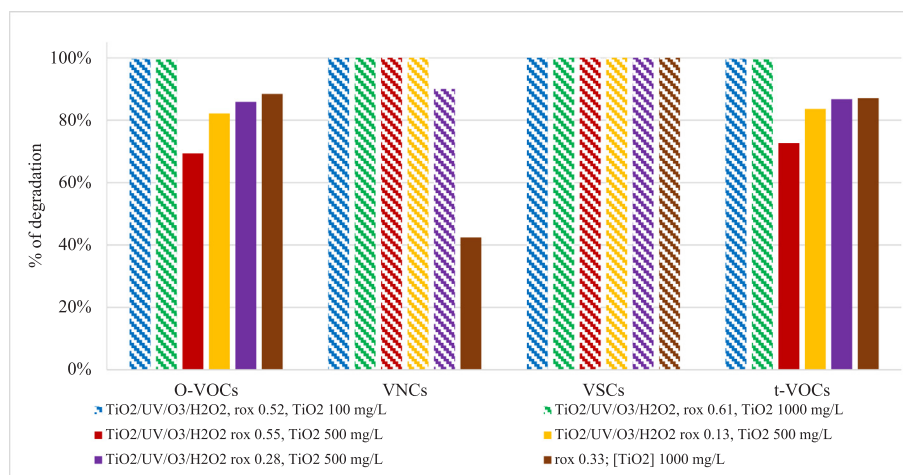


Fig. 8. t-VOCs, O-VOCs, VSCs, VNCs degradation after treatment in the  $\text{TiO}_2/\text{UV}/\text{O}_3/\text{H}_2\text{O}_2$  processes.

makes the measurement of turbidity under standard conditions impossible – the results are above the scale of the instrument. Still, as proved the studies of this paper, it is possible to increase the degradation effectiveness by application of UV light as well as  $\text{TiO}_2$ . However, the turbidity of the effluents is a one of the most important limiting criteria of the photocatalytic processes in this case. Summarizing, till some limiting level, the addition of  $\text{TiO}_2$  increases the process effectiveness, after that further addition of  $\text{TiO}_2$  (that increases the turbidity) can affect the efficacy of the UV, leading to the generation of less reactive species than  $\text{HO}^\cdot$ . With the lack of efficacy of UV and  $\text{TiO}_2$ , it remains as the main reaction pathway, i.e. the reaction with the oxidants in basic pH. Here,  $\text{H}_2\text{O}_2$  at basic pH cannot generate  $\text{HO}^\cdot$  and can explain why the decrease was more significant. Furthermore, the presence of  $\text{HO}^\cdot$  scavengers like carbonates, bicarbonates and sulfur ions can also explain the lower  $k$  values.

### 3.4. Sulfide ions monitoring

Analyzing Table 2 it is clear that sulfide ions concentration was completely depleted, achieving values below LOD (0.0032 mg/L) in all processes and at the first 30 min of treatment. This suggests that the sulfide ions were oxidized to sulfite or further to sulfate [69,70], much less dangerous/hazardous compounds and not harmful for biological technologies. Preliminary studies performed by ion chromatography for this project (data not shown) confirmed this pathway. This monitoring is very important due to the nature of the bitumen effluents. They contain significant concentration of sulfide ions which if the pH is corrected to neutral/acidic before treatment of the effluents,  $\text{H}_2\text{S}$  can be released [20], having a significant negative impact into environment and can lead to corrosion in to the stream pipelines of the industrial facility. All technologies including non-catalytic and non-irradiated processes can offer a pre-treatment before using AOPs like Fenton related technologies which are effective especially at neutral/acidic values.

### 3.5. Biodegradability

It is well known that the biodegradability is an important factor to determine the possibility of using biological technologies in certain wastewaters. This parameter is determined by the ratio between  $\text{BOD}_5$  and COD and the larger the value, the higher the quality of the treated effluent to be treated by biological techniques. Literature states clearly that a biodegradability higher or equal to 0.3 or 0.4 is enough for the biological technology, for instance activated sludge, to be operational and effective [71,72]. Table 2 exhibit the biodegradability before and after treatment for the non-catalytic and photocatalytic processes. It is

clear that the biodegradability index from the effluent was around 0.30 and 0.40. The technologies studied led to a small decrease in the biodegradability around 0.05 in the generality of the experiments. Nevertheless, the biodegradability after treatment was around 0.30 and 0.40, which is still biodegradable by biological approaches. Experiments 14, 19 and 29 were the only processes in which the biodegradability increased after treatment, with the exp. 14 with the most significant increase (0.28 to 0.37). Interestingly, the sole use of UV (exp. 29) increase, yet a small, in the biodegradability. The small amount of the COD oxidized by the UV light can be converted to  $\text{BOD}_5$ , improving the biodegradability of the treated effluent. These parameter proves that in fact the technologies used, especially the  $\text{TiO}_2/\text{UV}/\text{O}_3/\text{H}_2\text{O}_2$ , can sustain the application of biological technologies, like activated sludge for example.

### 3.6. Economic analysis

One of the crucial factors when studying a technology to implement in a real case scenario is the economic impact of the technology in the industrial process. The ideal technology must be effective, cheap and easy to implement, in order to reduce the economical and operational impact in the industrial plant. To check if the technologies studied in this work can be applied in an industrial plant, an economic evaluation was performed. The processes selected to perform the economic analysis were the processes that reached at least 25% of COD reduction, (exp. no. 8, 12, 14, 19, 24, 26–28, Table 1). The followed methodology was similar to our previous work [73], where it was calculated the cost of operation of each technology. It was set the milestone of 50% of COD reduction for all processes chosen to establish an appropriate comparison. The time of treatment needed to reach 50% of COD reduction was predicted using the reaction rate constant of each experiment, determined by standard procedures. The amount of oxidant needed to reach the milestone was determined by the oxidant flowrate and the treatment time. The prices of the chemicals were assumed taking into consideration the actual market:  $\text{H}_2\text{O}_2$  (30% v/v) has a market price of 500 American Dollars (\$) per ton and  $\text{TiO}_2$  a market price of 3000 \$ per ton [74,75]. In Poland, the price of electricity to industrial customers is around 0.11 \$/kWh (3600 kJ). The ozone generator, oxidant pump and UV lamp have working powers of 450, 80 and 250 W respectively.

Table 3 summarizes the main results of the operational costs of each process chosen to treat 1  $\text{m}^3$  of the bitumen effluents. The operational cost is the sum of the energy and chemical cost (Eq. (8)). The chemical cost is equal to sum of the cost of  $\text{TiO}_2$  and  $\text{H}_2\text{O}_2$ . The cost of  $\text{O}_3$  is zero because it is produced from dry air. Also the energy cost is the sum of the energy needed for  $\text{O}_3$  and  $\text{H}_2\text{O}_2$  processes and the energy needed for the UV processes. Each energy cost is determined using the treatment

**Table 3**

Main results to calculate the operational costs to treat 1  $\text{m}^3$ .

No.	Process	$k$ ( $\text{min}^{-1}$ )	treatment time (min)	Oxidant amount (kg)	catalyst amount (kg)	energy demand (kJ)	Chemical cost			Energy cost			Operational cost (\$/ $\text{m}^3$ )
							Cost of $\text{O}_3$ (\$)	Cost of $\text{H}_2\text{O}_2$ (\$)	Cost of $\text{TiO}_2$ (\$)	Cost of $\text{O}_3$ (\$)	Cost of $\text{H}_2\text{O}_2$ (\$)	Cost of UV (\$)	
26	$\text{H}_2\text{O}_2/\text{UV}$	9.0E-04	770	33	–	3049.8	–	16	–	–	23	71	110
8	$\text{TiO}_2/\text{O}_3/\text{UV}$	1.4E-03	495	20	0.5	4158.9	–	–	1.5	82	–	45	129
12	$\text{TiO}_2/\text{O}_3/\text{UV}$	1.0E-03	693	22	0.5	5822.4	–	–	1.5	114	–	64	179
24	$\text{O}_3/\text{UV}$	9.0E-04	770	32	–	6469.4	–	–	–	127	–	71	198
14	$\text{TiO}_2/\text{O}_3/\text{H}_2\text{O}_2/\text{UV}$	9.0E-04	770	$\text{O}_3: 19$ $\text{H}_2\text{O}_2: 6$	0.1	7208.7	–	3	0.3	127	23	71	223
19	$\text{TiO}_2/\text{O}_3/\text{H}_2\text{O}_2/\text{UV}$	1.6E-03	433	$\text{O}_3: 14$ $\text{H}_2\text{O}_2: 4$	0.5	4054.9	–	2	1.5	71	13	40	127
27	$\text{O}_3/\text{H}_2\text{O}_2$	1.0E-03	693	$\text{O}_3: 22$ $\text{H}_2\text{O}_2: 7$	–	4408.4	–	3	–	114	20	–	138
28	$\text{O}_3/\text{H}_2\text{O}_2/\text{UV}$	1.2E-03	578	$\text{O}_3: 19$ $\text{H}_2\text{O}_2: 6$	–	5406.5	–	3	–	95	17	53	168

time, the power of each equipment needed and the cost of the energy.

$$\text{Operationalcost} = \text{Chemicalcost} + \text{Energycost} \quad (8)$$

Comparing O<sub>3</sub> technologies with O<sub>3</sub>/H<sub>2</sub>O<sub>2</sub> technologies, it is clear that the O<sub>3</sub>/H<sub>2</sub>O<sub>2</sub> related processes were cheaper than O<sub>3</sub> related technologies. This is related with the time of treatment needed that is lower in O<sub>3</sub>/H<sub>2</sub>O<sub>2</sub> technologies. It follows from the synergistic effect of simultaneous injection of ozone and hydrogen peroxide (peroxone process). When the TiO<sub>2</sub> was added to the O<sub>3</sub>/UV system the operational cost decreased significantly (by 35%) from \$198 to \$129/m<sup>3</sup>. The same behavior occurred in the O<sub>3</sub>/H<sub>2</sub>O<sub>2</sub> technologies. The addition of the TiO<sub>2</sub> to the O<sub>3</sub>/H<sub>2</sub>O<sub>2</sub>/UV system had a significant decrease in the operational cost by 24% from \$168 to \$127/m<sup>3</sup>. In overall the cheapest process studied was H<sub>2</sub>O<sub>2</sub>/UV process (exp. 26) with \$110/m<sup>3</sup>. This process takes more time to achieve the goal than TiO<sub>2</sub>/UV/O<sub>3</sub>/H<sub>2</sub>O<sub>2</sub> process, which means that the residence time inside the reactor is higher and consequently a reactor with higher volume is needed to be used in the treatment process for same feedstock (fixed volumetric flowrate), therefore increasing the investment cost. Thus, TiO<sub>2</sub>/UV/O<sub>3</sub>/H<sub>2</sub>O<sub>2</sub> (exp. 19) with a comparable operational cost of \$127/m<sup>3</sup> can be taken into account as a reasonable alternative to H<sub>2</sub>O<sub>2</sub>/UV. Literature review regarding the studied photocatalytic processes applied in petroleum & refinery effluents was conducted in terms of cost evaluation. Several studies were performed in this field but without any cost analysis, thus proper comparison with other studies cannot be performed. Nevertheless, previous work based on the same technologies using a model WW containing selected VOCs revealed that TiO<sub>2</sub>/UV/O<sub>3</sub> was the optimal process, with TiO<sub>2</sub>/UV/O<sub>3</sub>/H<sub>2</sub>O<sub>2</sub> also having satisfactory results. In case of model effluents, the cost was almost 6 times lower. This indicates the importance of studies performed for real effluents where its more complex matrix strongly affects the obtained effectiveness and time of treatment.

This paper included also an alternative purpose of treatment. If the goal is to degrade only the sulfide ions, the most economic process is H<sub>2</sub>O<sub>2</sub>/UV (exp. 26) with an operational cost of only \$6/m<sup>3</sup> (Table 6S). Thank to solving out the issue of presence of sulfide ions this approach allows to further implement other very effective AOPs like Fenton related processes at a pH corrected to acidic.

Looking to the energy and operational cost, the economic analysis reveals that the energy cost plays a detrimental role with more than 80% of the operational cost. This means that these technologies are highly energy dependent. Since the effluent is generated in a refinery industry, in many cases, the industrial plant has an excess of energy (many refineries sell outside the electric energy), from recovery boilers or during the vapor production and therefore it is possible that the energy can be supplied by the facility itself rather than buying it from the national electric power system. This would decrease dramatically the operational cost of treatment, driving to conclusion that in this case the TiO<sub>2</sub>/UV/O<sub>3</sub>/H<sub>2</sub>O<sub>2</sub> is the optimal treatment process. A negative outcome from the photocatalytic system is related with the fact that further equipment is needed to separate the treated effluent from the catalyst, i.e. sedimentation tank or ultrafiltration system, but these separation processes are well established and do not state an issue at industrial scale. Nevertheless, TiO<sub>2</sub>/UV/O<sub>3</sub>/H<sub>2</sub>O<sub>2</sub> revealed to be promising technology to attempt scale up to a pilot scale in a real case scenario as a pre-treatment stage before the biological treatment stage.

### 3.7. Statistical approach for method optimization

In order to determine the optimal conditions for wastewater treatment and to examine the impact of individual conditions on the reduction of total parameters, multiple linear regression (MLR) followed by optimizer regression were used. MLR was used to determine the overall fit of the model and to describe how a single response variable Y (summary parameters – COD; BOD; sulfide ions content; total content of O-VOCs; total content of VNCs; total content of VSCs; overall total

content of VOCs;) depends linearly on a number of predictor variables X1-X6 (r<sub>ox</sub>; treatment time; application of UV; TiO<sub>2</sub> dose; application of H<sub>2</sub>O<sub>2</sub>; application of O<sub>3</sub> - respectively). A range of variable values used for the model is presented in Table 7S. A design matrix with response for reduction of summary parameters is summarized in Table 8S.

The analysis of variance (ANOVA) was used to evaluate the data. In ANOVA, the statistical F- and p-values were adopted as criteria at a 90% confidence level. The variables for which the p-value less than 0.1 were considered as statistically significant and having a substantial effect on the regression model. As shown in Tables 9S–15S, the regression model was found to be significant, with a p-value less than 0.052 and F-value in range from 3.37 to 16.09 for all summary parameters.

The response Eqs. (9)–(15) obtained for experimental results can be expressed as follow:

$$Y_{(\text{COD reduction})} = 9,40 + 29,33X_1 - 0,0374X_2 + 3,42X_3 + 0,00577X_4 + 4,82X_5 + 13,22X_6 \quad (9)$$

$$Y_{(\text{BOD reduction})} = 39,1 + 46,5X_1 - 0,1298X_2 + 3,3X_3 - 0,0072X_4 + 4,20X_5 + 15,8X_6 \quad (10)$$

$$Y_{(\text{S}^{2-}\text{reduction})} = 89,4 + 91,4X_1 - 0,1993X_2 - 2,11X_3 + 0,0008X_4 + 9,68X_5 + 35,68X_6 \quad (11)$$

$$Y_{(\text{O-VOCs})} = 0,353 + 0,494X_1 - 0,001171X_2 + 0,0662X_3 - 0,000030X_4 + 0,0886X_5 + 0,5723X_6 \quad (12)$$

$$Y_{(\text{VNCs})} = 0,715 + 0,647X_1 - 0,002130X_2 + 0,328X_3 + 0,000027X_4 + 0,0349X_5 + 0,2281X_6 \quad (13)$$

$$Y_{(\text{VSCs})} = 0,971 + 0,515X_1 - 0,001334X_2 - 0,0751X_3 + 0,000018X_4 + 0,0635X_5 + 0,2014X_6 \quad (14)$$

$$Y_{(\text{t-VOCs})} = 0,391 + 0,527X_1 - 0,001163X_2 + 0,0781X_3 - 0,000066X_4 + 0,0858X_5 + 0,5350X_6 \quad (15)$$

The equations explain the influence of the studied variables on the reduction of summary parameters. The regression model presented a high determination coefficient (R<sup>2</sup>) is within range from 55.94 to 87.34% along with the values of adjusted determination coefficient (R<sub>adj</sub><sup>2</sup>) in range from 32.65 to 81.91%. The obtained results indicate a good correlation between the experimental data and good fitting of the model.

In order to determine optimal variable values, in the first stage the minimum, maximum, and target values (i.e. total degradation) of individual summary parameters were selected (Table 16S).

In this study, a composite desirability (D) was used to identify the combination of variable settings that jointly optimize a set of summary parameters responses. The composite desirability combines the individual desirability of all the response variables into a single measure. Greater emphasis is placed on the response variables with the greatest importance. As shown in Table 9S–15S, statistically significant parameters (p-value lower than 0.1) affecting studied parameters are:

- in respect to COD reduction the variables X1 (r<sub>ox</sub>), X6 (application of ozone as oxidant),
- for BOD reduction: X1(r<sub>ox</sub>)
- for VNCs: X1(r<sub>ox</sub>), X2 (treatment time), X3 (application of UV light), X6 (application of ozone as oxidant);
- in respect to S<sup>2-</sup> reduction, O-VOCs degradation, VSCs degradation and tVOCs: X1(r<sub>ox</sub>), X2 (treatment time), X6 (application of ozone as oxidant).

The D values close to 1 indicate that the settings achieve favorable results for all responses, zero indicates that one or more responses are

outside their acceptable limits. For the proposed model, the composite desirability is 0.9694 which demonstrate the high relative importance of the responses.

The optimum process defined by presented approach is  $\text{TiO}_2/\text{UV}/\text{O}_3/\text{H}_2\text{O}_2$  performed at  $r_{\text{ox}}$  of 0,61 and  $\text{TiO}_2$  dose of 899 mg/L for 240 min. The optimization plot with fitted values for the predictor settings is presented on Fig. 6S.

It should be highlighted that statistical evaluation of data and its optimization is an useful approach, however in case of complex dependencies between several parameters studied it is not able to fully evaluate the effect of each parameters. A good example of such a case is visible for peroxone processes (combined application of hydrogen peroxide and ozone). The MLR approach used in this paper didn't indicate the advantages of peroxone process in comparison to sole use of ozone, but indeed this synergism is clearly visible from the obtained data. That is why the optimized by point-to-point experimental method  $r_{\text{ox}}$  revealed to be much lower than the one predicted by the model. Secondly, this studies revealed that there is a limiting amount of  $\text{TiO}_2$  that increases the degradation effectiveness. Exceeding this level causes significant drop in degradation performance – it follows from increasing turbidity which after the optimal catalyst dose inhibit the effect of UV light. Thus, in overall, it can be stated that such an statistical approach is useful to determine general dependencies, but final “tuning” of the method must be based on point-to-point optimization with second level of research planning allowing application of deep knowledge on the chemistry of applied AOPs.

#### 4. Conclusions

The studies revealed, that the developed technology can be implemented in two alternative scenarios – one when the goal is to maximize the degradation effectiveness and second one where the main goal is to degrade sulfide ions allowing to perform further treatment in a corrected pH values from the primary strongly basic pH.

A good synergism was confirmed for the approach of combining  $\text{TiO}_2$  with UV and the oxidants studied. It was proved that the matrix of the real WW studied influences negatively the degradation rate of the generality of the VOCs studied (k values) comparing to treatment of model effluents.

In all processes studied the sulfide ions were oxidized completely in the first 30 min of treatment, which eliminates the risk of  $\text{H}_2\text{S}$  formation and its emission to the atmosphere in case of effluents pH lowering. The biodegradability of the treated effluents did not change significantly with values around 0.3 and 0.4 of the treated effluents. On the basis of this value the compounds present in the effluents can be considered as biodegradable. Compounds like 1-propanol, furfural, cyclohexanol and cyclohexanone were persistent to degradation via  $\text{HO}^\cdot$  and were not degraded below the LOD in any process studied. The addition of the  $\text{TiO}_2$  decreases the operational cost of the  $\text{O}_3$  and  $\text{O}_3/\text{H}_2\text{O}_2$  related technologies.

The optimal process was  $\text{TiO}_2/\text{UV}/\text{O}_3/\text{H}_2\text{O}_2$ . The selection is based on low consumption of oxidant ( $r_{\text{ox}}$  of 0.28) and 500 mg/L of  $\text{TiO}_2$  with 38% of COD reduction, 84% of t-VOCs degradation and an operation cost of \$127/ $\text{m}^3$ . It exceeds by over 30% the theoretical value of COD reduction, based on the  $r_{\text{ox}}$ , proving the importance of the photocatalytic technology.

Furthermore, if the goal is to degrade sulfide ions, the cheapest in the comparison is the  $\text{H}_2\text{O}_2/\text{UV}$  process (exp.26) with total cost of only \$6.4/ $\text{m}^3$  of effluent, with a decrease of COD and t-VOCs by 19% and 24% respectively.

These technologies are promising as a pre-treatment stage before a second chemical treatment process or biological treatment stage, where toxic compounds are effectively degraded and the probability of  $\text{H}_2\text{S}$  formation was avoided. Thus, such technologies should be further studied at a pilot scale in a real case scenario, to evaluate if whether a second chemical or biological treatment in combination with the

studied technology can reach a high quality of treated effluent capable to be discharge without harmful consequences to the environment. Besides future studies on this technology at pilot scale treatment unit, the research should also include studies on implementation of available AOPs based on modified titanium dioxide with increased effectiveness in visible light, allowing successive lowering of the costs associated with energy consumption. The comparison of catalyst costs (modified  $\text{TiO}_2$ ) versus energy costs for such processes remains an open case.

#### Declaration of Competing Interest

The authors declare that they have no known competing financial interests or personal relationships that could have appeared to influence the work reported in this paper.

#### Acknowledgment

The authors gratefully acknowledge the financial support from the National Science Centre, Warsaw, Poland – decision no. DEC-2013/09/D/ST8/03973 and UMO-2017/25/B/ST8/01364.

The authors gratefully acknowledge the Evonik Industries for kindly providing the AEROXIDE®  $\text{TiO}_2$  P 25 Titanium dioxide.

The authors gratefully acknowledge the ICSO Chemical Production, Poland, for providing the STRUKTOL SB 2032, antifoam agent.

The authors gratefully acknowledge the Lotos Asphalt, Ltd. (Grupa Lotos) for their cooperation on this project.

#### Appendix A. Supplementary data

Supplementary data to this article can be found online at <https://doi.org/10.1016/j.cej.2019.123488>.

#### References

- [1] A.L.N. Mota, L.F. Albuquerque, L.T.C. Beltrame, O. Chivone-Filho, C.A.O. Nascimento, Advanced oxidation processes and their application in the petroleum industry: a review, Br. J. Pet. Gas. 2 (2009) 122–142 <http://www.portalabpg.org.br/bjpg/index.php/bjpg/article/view/57>.
- [2] F. Autelitano, F. Giuliani, Analytical assessment of asphalt odor patterns in hot mix asphalt production, J. Clean. Prod. 172 (2018) 1212–1223, <https://doi.org/10.1016/j.jclepro.2017.10.248>.
- [3] G. Boczkaj, A. Przyjazny, M. Kamiński, Characteristics of volatile organic compounds emission profiles from hot road bitumens, Chemosphere 107 (2014) 23–30, <https://doi.org/10.1016/j.chemosphere.2014.02.070>.
- [4] G. Boczkaj, A. Przyjazny, M. Kamiński, New procedures for control of industrial effluents treatment processes, Ind. Eng. Chem. Res. 56 (2014) 1503–1514.
- [5] I. Ben Hariz, A. Halleb, N. Adhoum, L. Monser, Treatment of petroleum refinery sulfidic spent caustic wastes by electrocoagulation, Sep. Purif. Technol. 107 (2013) 150–157, <https://doi.org/10.1016/j.seppur.2013.01.051>.
- [6] C.E. Santo, V.J.P. Vilar, C.M.S. Botelho, A. Bhatnagar, E. Kumar, R.A.R. Boaventura, Optimization of coagulation–flocculation and flotation parameters for the treatment of a petroleum refinery effluent from a Portuguese plant, Chem. Eng. J. 183 (2012) 117–123, <https://doi.org/10.1016/j.cej.2011.12.041>.
- [7] L. Yan, H. Ma, B. Wang, W. Mao, Y. Chen, Advanced purification of petroleum refinery wastewater by catalytic vacuum distillation, J. Hazard. Mater. 178 (2010) 1120–1124, <https://doi.org/10.1016/j.jhazmat.2010.01.104>.
- [8] G.T. Tellez, N. Nirmalakhandan, J.L. Gardea-Torresdey, Performance evaluation of an activated sludge system for removing petroleum hydrocarbons from oilfield produced water, Adv. Environ. Res. 6 (2002) 455–470, [https://doi.org/10.1016/S1093-0191\(01\)00073-9](https://doi.org/10.1016/S1093-0191(01)00073-9).
- [9] H.-H. Cheng, C.-C. Hsieh, Removal of aromatic volatile organic compounds in the sequencing batch reactor of petroleum refinery wastewater treatment plant, CLEAN – Soil Air Water 41 (2013) 765–772, <https://doi.org/10.1002/clean.201100112>.
- [10] A. Coelho, A.V. Castro, M. Dezotti, G.L. Santana, Treatment of petroleum refinery sourwater by advanced oxidation processes, J. Hazard. Mater. 137 (2006) 178–184, <https://doi.org/10.1016/j.jhazmat.2006.01.051>.
- [11] K.H. Kim, S.K. Ihm, Heterogeneous catalytic wet air oxidation of refractory organic pollutants in industrial wastewaters: a review, J. Hazard. Mater. 186 (2011) 16–34, <https://doi.org/10.1016/j.jhazmat.2010.11.011>.
- [12] M. Mehrjoui, S. Müller, D. Möller, A review on photocatalytic ozonation used for the treatment of water and wastewater, Chem. Eng. J. 263 (2015) 209–219, <https://doi.org/10.1016/j.cej.2014.10.112>.
- [13] S.-Y. Lee, S.-J. Park,  $\text{TiO}_2$  photocatalyst for water treatment applications, J. Ind. Eng. Chem. 19 (2013) 1761–1769, <https://doi.org/10.1016/j.jiec.2013.07.012>.
- [14] S. Munirasu, M.A. Haija, F. Banat, Use of Membrane technology for oil field and

- refinery produced water treatment—A review, *Process Saf. Environ. Prot.* (2016), <https://doi.org/10.1016/j.psep.2016.01.010>.
- [15] M. Bahri, A. Mahdavi, A. Mirzaei, A. Mansouri, F. Haghighat, Integrated oxidation process and biological treatment for highly concentrated petrochemical effluents: a review, *Chem. Eng. Process. - Process Intensif.* 125 (2018) 183–196, <https://doi.org/10.1016/j.cep.2018.02.002>.
- [16] M.K. Vineyard, Method and apparatus for pretreatment of wastewater streams by chemical oxidation, US patent 09/902,747, 2003.
- [17] G. Boczkaj, P. Makoś, A. Fernandes, A. Przyjazny, New procedure for the control of the treatment of industrial effluents to remove volatile organosulfur compounds, *J. Sep. Sci.* 39 (2016) 3946–3956, <https://doi.org/10.1002/jssc.201600608>.
- [18] G. Boczkaj, P. Makoś, A. Przyjazny, Application of dispersive liquid-liquid micro-extraction and gas chromatography-mass spectrometry (DLLME-GC-MS) for the determination of oxygenated volatile organic compounds in effluents from the production of petroleum bitumen, *J. Sep. Sci.* 39 (2016) 2604–2615.
- [19] G. Boczkaj, P. Makoś, A. Fernandes, A. Przyjazny, New procedure for the examination of the degradation of volatile organonitrogen compounds during the treatment of industrial effluents, *J. Sep. Sci.* (2017) 1–9, <https://doi.org/10.1002/jssc.201601237>.
- [20] M. Talei, D. Mowla, F. Esmaeilzadeh, Ozonation of an effluent of oil refineries for COD and sulfide removal, *Desalin. Water Treat.* 56 (2015) 1648–1656, <https://doi.org/10.1080/19443994.2014.951968>.
- [21] G. Boczkaj, A. Fernandes, P. Makoś, Study of different advanced oxidation processes for wastewater treatment from petroleum bitumen production at basic pH, *Ind. Eng. Chem. Res.* 56 (2017) 8806–8814, <https://doi.org/10.1021/acs.iecr.7b01507>.
- [22] A. Fernandes, P. Makos, G. Boczkaj, Treatment of bitumen post oxidative effluents by sulfate radicals based advanced oxidation processes (S-AOPs) under alkaline pH conditions, *J. Clean. Prod.* 195 (2018) 374–384, <https://doi.org/10.1016/j.jclepro.2018.05.207>.
- [23] L.F. Liotta, M. Gruttadauria, G. Di Carlo, G. Perrini, V. Librando, Heterogeneous catalytic degradation of phenolic substrates: catalysts activity, *J. Hazard. Mater.* 162 (2009) 588–606, <https://doi.org/10.1016/j.jhazmat.2008.05.115>.
- [24] A.R. Ribeiro, O.C. Nunes, M.F.R. Pereira, A.M.T. Silva, An overview on the advanced oxidation processes applied for the treatment of water pollutants defined in the recently launched Directive 2013/39/EU, *Environ. Int.* 75 (2015) 33–51, <https://doi.org/10.1016/j.envint.2014.10.027>.
- [25] P. Saritha, C. Aparna, V. Himabindu, Y. Anjaneyulu, Comparison of various advanced oxidation processes for the degradation of 4-chloro-2 nitrophenol, *J. Hazard. Mater.* 149 (2007) 609–614, <https://doi.org/10.1016/j.jhazmat.2007.06.111>.
- [26] T.A. Kurniawan, L. Yanyan, T. Ouyang, A.B. Albadarin, G. Walker, BaTiO<sub>3</sub>/TiO<sub>2</sub> composite-assisted photocatalytic degradation for removal of acetaminophen from synthetic wastewater under UV-vis irradiation, *Mater. Sci. Semicond. Process.* 73 (2018) 42–50, <https://doi.org/10.1016/j.mssp.2017.06.048>.
- [27] M. Tammara, V. Fiandra, M.C. Mascolo, A. Salluzzo, C. Riccio, A. Lancia, Photocatalytic degradation of atenolol in aqueous suspension of new recyclable catalysts based on titanium dioxide, *J. Environ. Chem. Eng.* 5 (2017) 3224–3234, <https://doi.org/10.1016/j.jece.2017.06.026>.
- [28] J. Araña, E. Pulido Melián, V.M. Rodríguez López, A. Peña Alonso, J.M. Doña Rodríguez, O. González Díaz, J. Pérez Peña, Photocatalytic degradation of phenol and phenolic compounds. Part I. Adsorption and FTIR study, *J. Hazard. Mater.* 146 (2007) 520–528, <https://doi.org/10.1016/j.jhazmat.2007.04.066>.
- [29] E.S. Elmolla, M. Chaudhuri, Degradation of amoxicillin, ampicillin and cloxacillin antibiotics in aqueous solution by the UV/ZnO photocatalytic process, *J. Hazard. Mater.* 173 (2010) 445–449, <https://doi.org/10.1016/j.jhazmat.2009.08.104>.
- [30] M. Buyukada, Removal, potential reaction pathways, and overall cost analysis of various pollution parameters and toxic odor compounds from the effluents of turkey processing plant using TiO<sub>2</sub>-assisted UV/O<sub>3</sub> process, *J. Environ. Manage.* 248 (2019) 109298, <https://doi.org/10.1016/j.jenvman.2019.109298>.
- [31] N.S. Shah, J.A. Khan, M. Sayed, Z.U.H. Khan, A.D. Rizwan, N. Muhammad, G. Boczkaj, B. Murtaza, M. Imran, H.M. Khan, G. Zaman, Solar light driven degradation of norfloxacin using as-synthesized Bi<sub>3</sub>+ and Fe<sub>2</sub>+ co-doped ZnO with the addition of HSO<sub>5</sub><sup>-</sup>: toxicities and degradation pathways investigation, *Chem. Eng. J.* 351 (2018) 841–855, <https://doi.org/10.1016/j.cej.2018.06.111>.
- [32] J.A. Navio, M. Garcia Gómez, M.A. Pradera Adrian, J. Fuentes Mota, Partial or complete heterogeneous photocatalytic oxidation of neat toluene and 4-picoline in liquid organic oxygenated dispersions containing pure or iron-doped titania photocatalysts, *J. Mol. Catal. A: Chem.* 104 (1996) 329–339, [https://doi.org/10.1016/1381-1169\(95\)00155-7](https://doi.org/10.1016/1381-1169(95)00155-7).
- [33] M. Sayed, A. Arooj, N.S. Shah, J.A. Khan, L.A. Shah, F. Rehman, H. Arandiyani, A.M. Khan, A.R. Khan, Narrowing the band gap of TiO<sub>2</sub> by co-doping with Mn<sup>2+</sup> and Co<sup>2+</sup> for efficient photocatalytic degradation of enoxacin and its additional peroxidase like activity: a mechanistic approach, *J. Mol. Liq.* 272 (2018) 403–412, <https://doi.org/10.1016/j.molliq.2018.09.102>.
- [34] M. Sayed, M. Gul, N.S. Shah, J.A. Khan, Z. Ul, H. Khan, F. Rehman, A.R. Khan, S. Rauf, H. Arandiyani, C.P. Yang, In-situ dual applications of ionic liquid coated Co<sup>2+</sup> and Fe<sup>3+</sup> co-doped TiO<sub>2</sub>: superior photocatalytic degradation of ofloxacin at pilot scale level and enhanced peroxidase like activity for calorimetric biosensing, *J. Mol. Liq.* 282 (2019) 275–285, <https://doi.org/10.1016/j.molliq.2019.03.022>.
- [35] R. Darvishi, C. Soltani, M. Mashayekhi, M. Naderi, G. Boczkaj, S. Jorfi, M. Safari, Sonocatalytic degradation of tetracycline antibiotic using zinc oxide nanostructures loaded on nano-cellulose from waste straw as nanosonocatalyst, *Ultrason. - Sonochemistry.* 55 (2019) 117–124, <https://doi.org/10.1016/j.ulsonch.2019.03.009>.
- [36] D. Shahidi, R. Roy, A. Azzouz, Advances in catalytic oxidation of organic pollutants – Prospects for thorough mineralization by natural clay catalysts, *Appl. Catal. B Environ.* 174–175 (2015) 277–292, <https://doi.org/10.1016/j.apcatb.2015.02.042>.
- [37] J.M. Poyatos, M.M. Muñoz, M.C. Almericia, J.C. Torres, E. Hontoria, F. Osorio, Advanced oxidation processes for wastewater treatment: state of the art, *Water Air Soil Pollut.* 205 (2010) 187–204, <https://doi.org/10.1007/s11270-009-0065-1>.
- [38] S. Soltan, H. Jafari, S. Afshar, O. Zabihi, Enhancement of photocatalytic degradation of furfural and acetophenone in water media using nano-TiO<sub>2</sub>-SiO<sub>2</sub> deposited on cementitious materials, *Water Sci. Technol.* 74 (2016) 1689–1697, <https://doi.org/10.2166/wst.2016.343>.
- [39] B. Murtaza, N.S. Shah, M. Sayed, J. Ali, M. Imran, M. Shahid, Z. Ul, H. Khan, A. Ghani, G. Murtaza, N. Muhammad, M. Sha, N. Khan, Synergistic effects of bis-muth coupling on the reactivity and reusability of zerovalent iron nanoparticles for the removal of cadmium from aqueous solution, *Sci. Total Environ.* 669 (2019) 333–341, <https://doi.org/10.1016/j.scitotenv.2019.03.062>.
- [40] F.H. Margha, M.S. Abdel-Wahed, T.A. Gad-Allah, Nanocrystalline Bi<sub>2</sub>O<sub>3</sub>–B<sub>2</sub>O<sub>3</sub>–(MoO<sub>3</sub> or V<sub>2</sub>O<sub>5</sub>) glass-ceramic systems for organic pollutants degradation, *Ceram. Int.* 41 (2015) 5670–5676, <https://doi.org/10.1016/j.ceramint.2014.12.152>.
- [41] Y. Xu, J. Ai, H. Zhang, The mechanism of degradation of bisphenol A using the magnetically separable CuFe<sub>2</sub>O<sub>4</sub>/peroxymonosulfate heterogeneous oxidation process, *J. Hazard. Mater.* 309 (2016) 87–96, <https://doi.org/10.1016/j.jhazmat.2016.01.023>.
- [42] G. Li, Y. Lu, C. Lu, M. Zhu, C. Zhai, Y. Du, P. Yang, Efficient catalytic ozonation of bisphenol-A over reduced graphene oxide modified sea urchin-like α-MnO<sub>2</sub> architectures, *J. Hazard. Mater.* 294 (2015) 201–208, <https://doi.org/10.1016/j.jhazmat.2015.03.045>.
- [43] R. Mirzaee, R. Darvishi, C. Soltani, A. Khataee, G. Boczkaj, Combination of air-dispersion cathode with sacrificial iron anode generating Fe<sup>2+</sup> + Fe<sup>3+</sup> + 2O<sub>4</sub> nanostructures to degrade paracetamol under ultrasonic irradiation, *J. Mol. Liq.* 284 (2019) 536–546, <https://doi.org/10.1016/j.molliq.2019.04.033>.
- [44] N.S. Shah, J.A. Khan, M. Sayed, Z.U.H. Khan, H.S. Ali, B. Murtaza, H.M. Khan, M. Imran, N. Muhammad, Hydroxyl and sulfate radical mediated degradation of ciprofloxacin using nano zerovalent manganese catalyzed S<sub>2</sub>O<sub>8</sub><sup>2-</sup>, *Chem. Eng. J.* 356 (2019) 199–209, <https://doi.org/10.1016/j.cej.2018.09.009>.
- [45] X. Chen, W.-D. Oh, T.-T. Lim, Graphene- and CNTs-based carbocatalysts in per-sulfate activation: material design and catalytic mechanisms, *Chem. Eng. J.* 354 (2018) 941–976, <https://doi.org/10.1016/j.cej.2018.08.049>.
- [46] K.M. Lee, C.W. Lai, K.S. Ngai, J.C. Juan, Recent developments of zinc oxide based photocatalyst in water treatment technology: a review, *Water Res.* 88 (2016) 428–448, <https://doi.org/10.1016/j.watres.2015.09.045>.
- [47] R. Thiruvenkatachari, S. Vigneswaran, I.S. Moon, A review on UV/TiO<sub>2</sub> photocatalytic oxidation process, *Korean J. Chem. Eng.* 25 (2008) 64–72, <https://doi.org/10.1007/s11814-008-0011-8>.
- [48] R. Fagan, D.E. McCormack, D.D. Dionysiou, S.C. Pillai, A review of solar and visible light active TiO<sub>2</sub> photocatalysis for treating bacteria, cyanotoxins and contaminants of emerging concern, *Mater. Sci. Semicond. Process.* 42 (2016) 2–14, <https://doi.org/10.1016/j.mssp.2015.07.052>.
- [49] K. Nakata, A. Fujishima, TiO<sub>2</sub> photocatalysis: design and applications, *J. Photochem. Photobiol. C Photochem. Rev.* 13 (2012) 169–189, <https://doi.org/10.1016/j.jphotochemrev.2012.06.001>.
- [50] G. Boczkaj, A. Fernandes, Wastewater treatment by means of advanced oxidation processes at basic pH conditions: a review, *Chem. Eng. J.* 320 (2017) 608–633, <https://doi.org/10.1016/j.cej.2017.03.084>.
- [51] J. Schneider, M. Matsuoka, M. Takeuchi, J. Zhang, Y. Horiuchi, M. Anpo, D.W. Bahnemann, Understanding TiO<sub>2</sub> photocatalysis: mechanisms and materials, *Chem. Rev.* 114 (2014) 9919–9986, <https://doi.org/10.1021/cr500189z>.
- [52] R.L. Zioli, W.F. Jardim, Photocatalytic decomposition of seawater-soluble crude-oil fractions using high surface area colloid nanoparticles of TiO<sub>2</sub>, *J. Photochem. Photobiol. A Chem.* 147 (2002) 205–212, [https://doi.org/10.1016/S1010-6030\(01\)00600-1](https://doi.org/10.1016/S1010-6030(01)00600-1).
- [53] C. Chen, J. Yu, B.A. Yoza, Q.X. Li, G. Wang, A novel “wastes-treat-wastes” technology: role and potential of spent fluid catalytic cracking catalyst assisted ozonation of petrochemical wastewater, *J. Environ. Manage.* 152 (2015) 58–65, <https://doi.org/10.1016/j.jenvman.2015.01.022>.
- [54] J. Saïen, H. Nejadi, Enhanced photocatalytic degradation of pollutants in petroleum refinery wastewater under mild conditions, *J. Hazard. Mater.* 148 (2007) 491–495, <https://doi.org/10.1016/j.jhazmat.2007.03.001>.
- [55] J. Saïen, F. Shahrezaei, Organic pollutants removal from petroleum refinery wastewater with nano titania photocatalyst and UV light emission, *Int. J. Photoenergy* 2012 (2012) 1–5, <https://doi.org/10.1155/2012/703074>.
- [56] W.Z. Khan, I. Najeeb, M. Tuiyebayeva, Z. Makhtayeva, Refinery wastewater degradation with titanium dioxide, zinc oxide, and hydrogen peroxide in a photocatalytic reactor, *Process Saf. Environ. Prot.* 94 (2015) 479–486, <https://doi.org/10.1016/j.psep.2014.10.007>.
- [57] P. Stepnowski, E.M. Siedlecka, P. Behrend, B. Jastorff, Enhanced photo-degradation of contaminants in petroleum refinery wastewater, *Water Res.* 36 (2002) 2167–2172.
- [58] F. Shahrezaei, Y. Mansouri, A.A.L. Zinatizadeh, A. Akhbari, Process modeling and kinetic evaluation of petroleum refinery wastewater treatment in a photocatalytic reactor using TiO<sub>2</sub> nanoparticles, *Powder Technol.* 221 (2012) 203–212, <https://doi.org/10.1016/j.powtec.2012.01.003>.
- [59] D.A.D.A. Aljuboury, P. Palaniandy, H.B.A. Aziz, S. Feroz, S.S.A. Amr, Evaluating photo-degradation of COD and TOC in petroleum refinery wastewater by using TiO<sub>2</sub>/ZnO photo-catalyst, *Water Sci. Technol.* 74 (2016) 1312–1325, <https://doi.org/10.2166/wst.2016.293>.
- [60] J.J. Rueda-Márquez, I. Levchuk, I. Salcedo, A. Acevedo-Merino, M.A. Manzano, Post-treatment of refinery wastewater effluent using a combination of AOPs (H<sub>2</sub>O<sub>2</sub>

- photolysis and catalytic wet peroxide oxidation) for possible water reuse. Comparison of low and medium pressure lamp performance, *Water Res.* 91 (2016) 86–96, <https://doi.org/10.1016/j.watres.2015.12.051>.
- [61] S. Natarajan, H.C. Bajaj, R.J. Tayade, Recent advances based on the synergetic effect of adsorption for removal of dyes from waste water using photocatalytic process, *J. Environ. Sci. (China)* (2016) 1–22, <https://doi.org/10.1016/j.jes.2017.03.011>.
- [62] J. Fenoll, M. Martínez-Menchón, G. Navarro, N. Vela, S. Navarro, Photocatalytic degradation of substituted phenylurea herbicides in aqueous semiconductor suspensions exposed to solar energy, *Chemosphere* 91 (2013) 571–578, <https://doi.org/10.1016/j.chemosphere.2012.11.067>.
- [63] U.I. Gaya, A.H. Abdullah, M.Z. Hussein, Z. Zainal, Photocatalytic removal of 2,4,6-trichlorophenol from water exploiting commercial ZnO powder, *Desalination* 263 (2010) 176–182, <https://doi.org/10.1016/j.desal.2010.06.055>.
- [64] M. Litter, Introduction to photochemical advanced oxidation processes for water treatment, in: P. Boule, D.W. Bahnemann, P.K.J. Robertson (Eds.), *Environ. Photochem. Part II*, Springer Berlin Heidelberg, 2005, pp. 325–366, <https://doi.org/10.1007/b89482>.
- [65] H. Zangeneh, L. Zinatizadeh, M. Feizy, A comparative study on the performance of different advanced oxidation processes (UV/O<sub>3</sub>/H<sub>2</sub>O<sub>2</sub>) treating linear alkyl benzene (LAB) production plant's wastewater, *J. Ind. Eng. Chem.* 20 (2014) 1453–1461, <https://doi.org/10.1016/j.jiec.2013.07.031>.
- [66] P.S. Thind, D. Kumari, S. John, TiO<sub>2</sub>/H<sub>2</sub>O<sub>2</sub> mediated UV photocatalysis of chlorpyrifos: optimization of process parameters using response surface methodology, *J. Environ. Chem. Eng.* (2017), <https://doi.org/10.1016/j.jece.2017.05.031>.
- [67] B. Ohtani, S.-W. Zhang, S. Nishimoto, T. Kagiya, Catalytic and photocatalytic decomposition of ozone at room temperature over titanium (IV) oxide, *J. Chem. Soc., Faraday Trans.* 88 (1992) 1049, <https://doi.org/10.1039/ft9928801049>.
- [68] A. Fernandes, M. Gagol, P. Makoś, J.A. Khan, G. Boczkaj, Integrated photocatalytic advanced oxidation system (TiO<sub>2</sub>/UV/O<sub>3</sub>/H<sub>2</sub>O<sub>2</sub>) for degradation of volatile organic compounds, *Sep. Purif. Technol.* 224 (2019) 1–14, <https://doi.org/10.1016/j.seppur.2019.05.012>.
- [69] A. Hawari, H. Ramadan, I. Abu-Reesh, M. Ouederni, A comparative study of the treatment of ethylene plant spent caustic by neutralization and classical and advanced oxidation, *J. Environ. Manage.* 151 (2015) 105–112, <https://doi.org/10.1016/j.jenvman.2014.12.038>.
- [70] M. Peleg, The chemistry of ozone in the treatment of water, *Water Res.* 10 (1976) 361–365, [https://doi.org/10.1016/0043-1354\(76\)90052-X](https://doi.org/10.1016/0043-1354(76)90052-X).
- [71] M. Gagol, A. Przyjazny, G. Boczkaj, Effective method of treatment of industrial effluents under basic pH conditions using acoustic cavitation – a comprehensive comparison with hydrodynamic cavitation processes, *Chem. Eng. Process. Process Intensif.* 128 (2018) 103–113, <https://doi.org/10.1016/j.cep.2018.04.010>.
- [72] G. Samudro, S. Mangkoedihardjo, Review on bod, cod and bod/cod ratio: a triangle zone for toxic, biodegradable and stable levels, *Int. Acad. Res.* 2 (2010) 235–239.
- [73] A. Fernandes, P. Makoś, J.A. Khan, G. Boczkaj, Pilot scale degradation study of 16 selected volatile organic compounds by hydroxyl and sulfate radical based advanced oxidation processes, *J. Clean. Prod.* 208 (2019) 54–64, <https://doi.org/10.1016/j.jclepro.2018.10.081>.
- [74] P.P. EUWID, Upward spiral in titanium dioxide prices slowing in second quarter, *EUWID Pulp Pap.* 20/2018. (2018). <https://www.euwid-paper.com/news/singlenews/Artikel/upward-spiral-in-titanium-dioxide-prices-slowing-in-second-quarter.html>. (accessed November 21, 2018).
- [75] P.P. EUWID, Titanium dioxide prices left untouched in Q3, *EUWID Pulp Pap.* 34/2018. (2018) 3. <https://www.euwid-paper.com/news/singlenews/Artikel/titanium-dioxide-prices-left-untouched-in-q3.html>. (accessed November 21, 2018).